Deanship of Graduate Studies
Al – Quds University

Assessing Heavy Metal Pollution in Soils of Regions from Palestine

Adel Abd Al Haleem Abd Al Hamid Bisher

M.Sc. Thesis

Jerusalem - Palestine

December -2016

Assessing Heavy Metal Pollution in Soils of Regions from Palestine

Prepared by

Adel Abd Al Haleem Abd Al Hamid Bisher

B.Sc: Alquds University, Palestine

Supervisors: **Dr. Salman M Salman**

Physics Department, Al Quds University, Palestine

Co-Supervisors **: Dr. Messaoud Harfouche**

Beamline Scientist, SESAME, Jordan

A thesis Submitted in Partial Fulfillment of Requirements for the Degree of Master of Science in Physics

Jerusalem - Palestine

December - 2016

Al Quds University
Deanship of Graduate Studies
Physics Department

Thesis Approval

Assessing Heavy Metal Pollution in Soils of Regions from Palestine

Prepared By: Adel Abd Al Haleem Abd Al Hamid
Registration No: 21310122

Supervisor: Dr. Salman M Salman
Co-Supervisor: Dr. Messaoud Harfouche

Master thesis submitted and accepted, Date:18/12/2016
The name and signature of examining committee member are as follows

1. Chairman of the Committee: Professor Salman M Salman
2. Internal Examiner: Professor Musa Abu Tair
3. External Examiner: Professor Mustafa Abu Safa

Jerusalem, Palestine
December -2016

Dedication

I dedicate this thesis to my family, especially to my Mother and father for their patience and understanding. To my brothers, and sisters for opening my eyes to the world.

To the soul that hugs my soul, to the heart that pours secrets in my heart, to the hand that lit my emotions, to faith that is considered the frame of my love, I present this Work.

Declaration

I hereby declare that this thesis is based on the results found by myself. Materials of works found by SESAME. This thesis, neither in whole or in part, has been previously submitted for any degree.

The work was done under the supervision of Dr. Salman M Salman, at Alquds University, Palestine, and Dr. Messaoud Harfouche, at SESAME, Jordan.

Signed ……

Adel Abd Al Haleem Abd Al Hamid Bisher

Date: 18/12/2016

The project is part of a collaborative effort between the SESAME Jordan, and al-Quds University, Palestine, coordinated Dr. Salman M. Salman from Physics at Alquds University and Dr. Messaoud Harfouche, at SESAME, Jordan.

Acknowledgements

First I wish to express my gratitude to the Almighty Allah for providing the grant to make this thesis possible.

Thanks and appreciation to my supervisor Dr. Salman M Salman who helped me through all stages of my studies and research and established the warm cooperation between Alquds University and SESAME.

Thanks to my supervisor Dr. Messaoud Harfouche for his guidance and support in providing the opportunity to acquire the needed skills and the help he made in facilitating the data tests in Jordan, and the XAFS test in Thailand. Dr. Harfouche was always ready to help whenever I ran in some problems.

Special thanks to SESAME for the hospitality and financial support of my visits, and to the staff for their technical and moral support and for providing resources and access to finalize this work. Thanks to Dr. Ma'moun Makahleh, Eng. Sukayna Jarrar, Eng. Khaled Karajeh and Eng. Muna Abu-Alsheikh, from The Jordanian Atomic Energy Commission (JAEC), for their efforts in running some experiments.

Appreciation to the Jordanian Atomic Energy Commission for providing access to the ICP-MS making important measurements of the trace elements concentrations.

Gratitude also goes to the Synchrotron Light Research Institute in Thailand, and the XAFS department staff for their help to run the XAFS Experiments using the BL8 (XAS).

Many thanks to my family and friends, especially to my friend Riyad M Jaber who stood beside me and encouraged me constantly and for his kind help and continuous support during my experimental work.

Adel Abd Al Haleem Abd Al Hamid Bisher

Abstract

Soil is a crucial component for rural and urban environments, and its wise management is the key to soil quality. In this work, heavy metals in soils from three regions in Palestine, Hebron, Qalqilia and Jericho, were analyzed to assess the impact of urbanization and industrialization on soil pollution. A number of soil samples were collected and analyzed for major heavy metals namely Chromium-Cr, Manganese-Mn, and Zinc-Zn. We used inductive coupled plasma–mass spectrometry (ICP-MS) to measure these trace elements concentrations.

Measurements revealed that Chromium and Zinc are present in concentrations higher than the maximum tolerated. Jericho sites are polluted by Cr with a concentration reaching 548 parts per million (ppm). Zn concentration averaged at 452 ppm. Qalqilia sites have slight Cr pollution with concentration of 110 ppm. Hebron samples did not measure any excess of the three element based on the World Health Organization standards. These results are not surprising taking into account the higher rate of irrigated agriculture in Jericho and Qalqilia where many minerals and pesticides are heavily used year around.

In addition, X-ray Absorption Fine Structure (XAFS) technique was used to investigate the local structural order around Mn, Cr and Zn in the soils samples. XAFS analysis revealed a presence of C and P ligands in the structure around Zn illustrating the **organic form of Zn.** In contrast, local structures around Cr revealed a presence of Mn atoms and thus Cr remains in its **inorganic form**. Cr is present in its trivalent oxidation form Cr (III) which minimizes mobility and limits harmfulness. Local structures around Mn revealed a presence of C and Mn atoms illustrating the **Mn organic form**. Mn is present in its trivalent and tetravalent oxidation forms Mn (III), Mn(IV) that also mobility and harmfulness.

We recommend extensive and systematic studies of the Palestinian lands concerning other metals and possible toxicants and a continuation of the study through the productive collaboration with SESAME.

Contents **page**

List of Tables

Chapter Two

Chapter Three

Chapter Four

List of Figures

Chapter 1

Chapter 2

Chapter 3

Chapter 4

List of Abbreviations and Symbols

A	Ampere
Å	Angstrom
[A]	Molar Concentration of A
℃	Degree Celsius
EDXS	Energy Dispersive X-ray Spectroscopy
EXAFS	Extended X-Ray Absorption Fine Structure
ICP-MS	Inductively coupled Plasma-Mass Spectroscopy
JAEC	Jordanian Atomic Energy Commission
Kcps	Killo Count Per second
keV	Killo electron volt
Log	Logarithm Base 10
L.O.I	Loss of Ignition
M	Molar Concentration
MAC	Maximum Allowable Concentration
MB	Burned Mass Sample
MD	Dry Mass Sample
MW	Wet Mass Sample
pH	Degree of Acidity or Basicity
POM	Particulate Organic Matter
ppm	Part Per Million
Q	Quartz
RSS	Royal Scientific Society
SEM	Scanning Electron Microscopy
SESAME	**S**ynchrotron-light for **E**xperimental **S**cience and **A**pplications in the **M**iddle **E**ast
SMC	Soil Moisture Content
SVOC	Soil Volatile Organic Content
SOM	Soil Organic Matter
XAFS	X-Ray Absorption Fine Structure
XANES	X-Ray Absorption Near Edge Spectroscopy

Part I
Review and Soils Characterizations

1 Introduction and Past Work

1.1 Introduction

1.1.1 Adsorption and Mobility of Heavy Metals

Heavy metals are found naturally in the earth, and become concentrated as a result of different factors including human related activities. Common sources are from mining and industrial wastes; vehicle emissions; lead-acid batteries; fertilizers, paints and treated woods. Characterizing the factors affecting bioavailability, leaching and toxicity of metals in soil is of paramount importance. Metals are significant natural components of all soils where their presence in the mineral fraction comprises a store of potentially mobile metal elements as important components of clays, minerals, iron and manganese oxides that, in turn, have a dramatic impact on soil geochemistry.

Metals are also present frequently in organic bound forms, with some metal recycling occurring as a result of organic matter decomposition. The aqueous phase provides a mobile medium for chemical reactions, metal transfer and circulation through the soil to organisms and the aquatic environment. Heavy metals can be involved in series of complex chemical and biological interactions. The most important factors which affect their mobility are pH, sorbent nature, presence and concentration of organic and inorganic ligands, including humic and fulvic acids, root exudates and nutrients. Furthermore, redox reactions, both biotic and abiotic, are of great importance in controlling the oxidation state and thus, the mobility and the toxicity of many elements, such as Cr, Mn, Co, Pb, Zn, Ni and Cu. Redox reactions can mobilize or immobilize metals, depending on the particular metal species and micro-environments [Violante et al, 2010].

Redox reactive metals often do have different degrees of toxicity depending on the specific metal oxidation state. For example, chromate is toxic to plants, animals and humans and is a

suspected carcinogen, whereas Cr(III) is not toxic to plants and necessary for animal nutrition. Hence reactions that reduce Cr(VI) to Cr(III) are of great importance. Furthermore, Cr(VI) is mobile in soils and readily available. Organic material, sulfides, and ferrous species appear to be the dominant reductants. Very stable Cr(III)-organic complexes form when Cr(VI) is reduced by soil organic matter [Fendorf, 1995].

Heavy metals accumulate in the sediments through complex physical and chemical adsorption mechanisms depending on the nature of the sediment matrix and the properties of the adsorbed compounds. Several processes lead to the association of heavy metals with solid phases, such as the direct absorption by fine-grained inorganic particles of clays; adsorption of hydrous ferric and manganic oxides which may in turn be associated with clays; adsorption on or complexation with natural organic substances, which may also be associated with inorganic particles, and direct precipitation as new solid phases [Senesi, 1992].

The adsorption process is influenced by several chemical–physical and chemical parameters such as: pH, oxidative–reductive potential, dissolved oxygen, organic and inorganic carbon content, and the presence in water phase of some anions and cations that can bind or co-precipitate the water-dissolved or suspended pollutants.

This study on interaction between soil constituents and heavy metals at different study scales are essential for an increased understanding of the fate and impacts of metal pollutants in soils. The goal of this study is to examine the characteristics of the heavy metals, their mobility and bindings in the soil matrix in order to understand the accumulation mechanism; and to study heavy metal pollutants in the fine-grained material of the sediments of three selected locations in Palestine.

The study combines conventional with advanced synchrotron-based techniques to examine the soil contaminants, their oxidation state and local structural behavior and hence understand their mobility and accumulation in the soil matrix. Mineralogical and geochemical studies on the heavy metals in Palestine will identify the dominant forms of emitted metals. Furthermore,

investigating the stability in alternating wet and dry soil conditions will be of great help to understand the contamination forms of heavy metals.

This research will utilize a combination of chemical extraction methods and spectroscopy to characterize the redox states and binding environment of heavy metals in the soil. In addition, we hope to understand the mechanisms behind the local structural environment of heavy metals using the conventional such as Inductively Coupled Plasma-Mass Spectroscopy ICP-MS and synchrotron based techniques like X-ray Absorption Fine Structure (XAFS).

XAFS spectroscopy became the method of choice for probing the specification of metal contaminations at the molecular level and it has demonstrated the variable reactivity and specification of heavy metals in model systems, soils and sediments. The utilization of XAFS and conventional techniques to study the structural behavior around heavy metals and toxic elements as contaminants and a pollutants of a soils have been the subject of many research works with some briefly described below.

1.1.2 Problem Statement

The soil contamination can be defined as the presence of man-made chemicals and materials that alter the natural soil conditions or it's environment. Alternatively, it can be described as the pollution caused by the presence of man-made toxic materials or chemicals in soils with high concentrations that can cause risk to human health and the earth ecosystems.

The contamination can affect the soil in many ways like, reducing fertility, crop yield, and the nitrogen fixation. They cause ecological imbalance, a dangerous effect to the groundwater, public health, and many problems to the earth ecology. Pollution can happen through discharge of industrial wastes including heavy metals from certain factories.

Cr, Mn and Zn are examples of heavy metals that can cause serious adverse effects if found in high concentrations- to the soil system and health, through the food intake route. Cr is specially highly toxic, if found in the hexavalent form Cr(VI).

Methods for soil contamination monitoring include chemical, geophysical, and biological techniques. Chemical techniques measure specific organic, inorganic, or radioactive contaminants in the soil using instruments such as a gas chromatograph, atomic absorption spectrometer, or mass spectrometer. Geophysical techniques examine changes in the soils physical properties and the contaminants to address large scale soil contamination. Biological techniques use organisms as indicators of soil contamination, or byproducts of contaminant biodegradation processes to monitor or predict changes of metals concentrations in soils over time [Aelion C. M, 2003].

Our study is one of few done in Palestine using XAFS techniques, to find the concentrations of high risk elements in soils from three areas in Palestine to determine the level of non-organic contaminations, especially Cr, Mn and Zn. It aims to measure the elements concentration using ICP-MS in addition to analyses of chemical configurations using XANES and EXAFS techniques.

Soil characterizations are done using conventional Soil Moisture Content (SCO), Soil Organic Content (SOC) and pH with comparisons between the three sites. The ICP-MS measurements were made at the Jordanian Atomic Energy Commission (JAEC) .

XAFS techniques are powerful tools for structural determinations of the oxidation states, coordination numbers, interatomic spacing's, and the nearest neighbor atoms of the elements of interest. Analyzing data in a synchrotron facility provides detailed information about the local structure and the occupied local electronic states too. XAFS refer to the details of how x-rays are absorbed by atoms at energies near and above the core-level their binding energies. They represent the modulation of atoms x-ray absorption probability due to chemical and physical states [Matthew Newville, 2004]. We used EXAFS and XANES in Beamline BL8 (XAS) at Synchrotron Light Research Institute, in Thailand.

1.1.3 Study Objectives

1. Perform conventional techniques to measure some natural parameters for our samples SMC, SOC and pH were measured.

2. Use XAFS, and derivatives including the XANES, and EXAFS to determine the soils elemental composition and availability, the physical and chemical properties, and the structural configurations of the elements of interest namely Cr, Zn and Mn. The measurements include the oxidation states, coordination numbers, interatomic spacing's, nearest neighbor's composition surrounding the target atoms.
3. Use ICP-MS to measure the trace concentrations of the elements, and compare the concentrations with the standard tolerant concentration limits. Hence determine the soils pollution levels, for different sites, locations and depths.
4. Introduce the synchrotron light sources techniques to enlarge the SESAME user's community where Palestine is one of the founding members.

1.1.4 SESAME Synchrotron [SESAME, 2016]

SESAME is an international organization run under the auspices of UNESCO and it is near completion in Allan-Jordan and scheduled to operate by middle of 2017. Its mission is to promote collaborations in the Middle East and the Mediterranean region for basic and applied research in physics, chemistry, biology, materials science, environmental, medical, archaeological studies, and other applications of relevance to the region. SESAME is open for members and international groups and offers research opportunities in a wide range of application for the academia and industry. Some SESAME attributes include a wide spectrum of synchrotron light ranging from infrared to hard X-rays and a mixture of straight sections (short, medium and long), allowing optimal use of a variety of undulators with flexible polarization schemes that can rapidly change it in the kHz range.

History of SESAME

SESAME is a third-generation machine and the Middle East's first major international research Centre. It is a cooperative venture by scientists and governments of the region set up on the model of CERN (European Organization for Nuclear Research). It is an autonomous intergovernmental organization for the service of Member States who have full control over policies, development, and financial matters. The formal status was established after the approval by the UNESCO Organization's Executive Board (164th session, May 2002), and the signing of its initiation by 6 founding members including Palestine.

SESAME is expected to foster scientific and technological excellence in the Middle East and neighboring countries that will help prevent or reverse the brain drain by enabling world-class scientific research many subjects and build scientific and cultural bridges between societies, and contribute to a culture of international cooperation in science.

Figure 1.1: External view of the main building of SESAME.

SESAME Machine: Microtron, Booster, Storage Ring

The accelerator complex consists of a 22 MeV electron pre-accelerator (Microtron), an 800 MeV electron booster synchrotron, and a 2.5 GeV electron accelerator and storage ring. The Microtron and Booster Synchrotrons are components of the donated BESSY I machine from Germany (Figure 1.2). The 2.5 GeV Storage Ring is completely new.

The electrons are emitted by the Microtron with energy of 22 MeV, and then accelerated in the booster until their energy reaches 800 MeV using pulsed electric field (Figure 1.2). The electrons are then transferred to the new storage ring and accelerated to reach the energy of 2.5 GeV. In the storage ring the electrons circulate at the target energy for many hours at 350000 cps. The electrons are grouped into punches, from 1 to 352 according to the operation of the machine.

Figure 1.2: Booster under assembly at SESAME.

Figure 1.3 shows a typical synchrotron facility with a variety of beamlines to study a wide range of materials and using equally wide range of photos energies from the very low infrared to the hard X-rays.

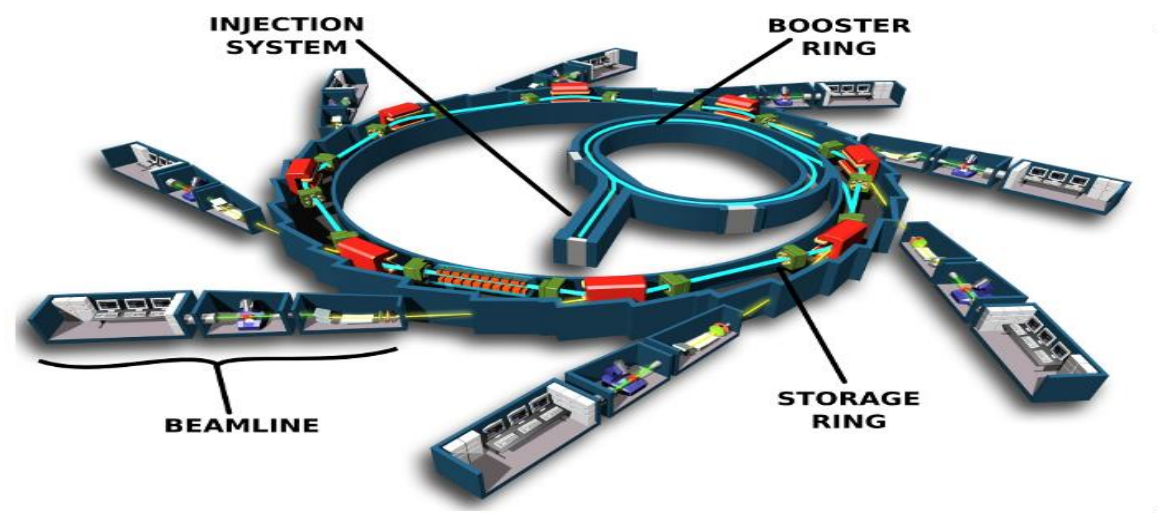

Figure1.3: A Schematic Diagram of a Synchrotron Facility

1.2 Past Work

[M. Harfouche, 2009] studied the structural behavior of Zn in agricultural soils polluted 100-50 years ago by metallurgical fallout and used for corn production. XAFS technique was the main tool used to evaluate how Zn is associated to Particulate Organic Matter (POM). Data revealed multiple and heterogeneous speciation of Zn. Small interactions from next-nearest

neighbors around Zn were observed. Combining micro-XRF and micro-XAFS synchrotron based-techniques showed that Zn is mainly located in POM matrix. Nevertheless, a residue of the Zn-distribution related to inorganic matter is present in the soil as franklinite-type mineral. [http://www.chemicalghosts.org].

[Andrej, 2002] used XANES multiple scattering mass spectroscopy approach with an example of Zn spectra. A comparison was made between the calculated and measured spectra of ZnO, indicated failures of the muffin-tin approximation. Further attempts were made to bring XANES analysis to a more quantitative level. The first step is to relax the muffin-tin shackles and other modifications may be more sophisticated.

[Gilberto, 2004] reviewed the EXAFS spectroscopy, which extracts structural information by analyzing the X-ray absorption spectra. A determination of neighboring atoms is confined to 4-8 Å radius from the element of interest.

[Guillaume, 1999] investigated a smelter contaminated soil from sites in France and the USA. They showed that bulk Pb concentration is 6000-10000 ppm at Leadville-France site. Because the samples were heterogeneous and multiphase mixtures, a variety of bulk analytical methods were used. They include some synchrotron-based techniques to enable identification of amorphous or nanocrystal line Pb-containing phases and the spatial distribution of Pb at a scale of 25mm. The combination of linear least-squares fitting of EXAFS data of complex multi-phase Pb-containing mixtures, and model compounds with conventional shell fitting of the data provides a semi-quantitative estimate of the various chemical forms of Pb in the multi-phase mixtures including adsorbed Pb. The most important result was providing direct evidence for adsorption, in determining the fate of Pb.

[Titian A, 2006] explained the speciation and solubility of heavy metals in contaminated soils, using X-ray micro-fluorescence, EXAFS Spectroscopy, chemical extraction, and thermodynamic calculations. They measured the solubility of Zn, Cu, and Pb and determined the nature and fractional amount of Zn in a near-neutral pH (6.5–7.0). In addition, the extractability of Zn, Cu and Pb with citrate, S-ethylenediaminedisuccinic acid (EDDS), and thylenediaminetetraacetic acid (EDTA) was measured as a function of time (24 h, 72 h, 144 h) and the number

of applications of the chelant (5 applications each with 24 h of contact time). Despite the long-term contamination of the soil, about 79% of Zn, 91% of Pb, and 100% of Cu could be soluble in the laboratory on a time scale of a few days by chemical complexants. According to metal speciation results and thermodynamic calculations, the lower extraction level measured for Zn is due to the Zn phyllosilicate, which is less soluble than Zn phosphate and Zn ferrihydrite

[Atsushi, 2012] Determined Pb speciation in fly ash by XAFS spectroscopy and a sequential extraction. They studied the chemical state of lead in fly ash generated from a thermally treated waste by measuring toxicity and solubility which depend on the elements chemical state. EXAFS, XANES and sequential Extraction methods were used to gain information about the lead chemical state in fly ash. It was not easy to measure the chemical composition using only EXAFS. XANES fitting analysis showed that $PbSiO_3$, $PbCl_2$, or $Pb_2O(OH)_2$ were the dominant chemical species in fly ash. The results of multiple analyses should be examined multilaterally to improve the accuracy of the final analysis. It is important to test if the chemical equilibrium model simulation, is consistent with the analytical approach.

[Frenkel, 2001] investigated Cu(II) in soil by X-ray absorption spectroscopy. The structural parameters of the Cu^{2+} target were measured for soils exposed to copper and eluted with 0.1 M HCl. Measurements were obtained using synchrotron sources of second and third generations machines. XANES indicated that the copper in both samples, is likely to be predominantly bound by oxygen-containing functional groups. EXAFS analysis showed that the equatorial Cu-O distances were similar to those seen for Cu^{2+}-humic complexes in aqueous solutions. The axial distances for both samples were longer than in water and this may indicate a type of ligation not similar to that in solutions. The mean square deviation of the axial Cu-O distance in the 0.1 M HCl eluted sample indicated a stronger bond compared with that in the sample containing both extractable and tightly bound copper.

[Jeffrey Lewi, 2010] used EXAFS analysis of Pb speciation in bullet-contaminated range soils. The lab-based study investigated a range of soils contaminated by 500 high velocities 7.62 mm jacketed Swedish military rounds. A 0.06 mm portion of the soil was analyzed using

EXAFS to determine the speciation of Pb both before and after a simulated springtime snow melting. Lead(II) Oxide (PbO) and not hydrocerrusite was the dominant lead species. This is due to the low organic content and pH of the soil in the site.

[Alian, 1996] showed that using conventional analytical techniques still face challenges in the direct determination of the chemical form of trace metals in soils. They used EXAFS to study the form of trace lead. Three soils contaminated by synthesis of lead organometallics for gasoline antiknocks, Pb-Zn smelting, and recycling of lead acid battery, were investigated. In the soil contaminated by alkyl-tetravalent lead compounds, lead was divalent and complexed to salicylate and catechol-type functional groups of humic substances. The lead sulfate and silica-bound lead are the predominant forms in the vicinity of the battery reclamation area. Near the smelter, lead was divalent and coordinated to Oxide (O^{2-} and hydroxide (OH^{-1}) ligands. The multiplicity of lead species in soils contaminated by smelting activities is expected to be the result of long-term atmospheric emissions and a variety of lead-containing phases, successively emitted in the atmosphere.

[Bashar M, 2001] applied Scanning Electron Microscopy (SEM) and Energy Dispersive X-ray Spectroscopy (EDX) mapping techniques. Different samples were compared. It provided X-ray counts from thousands of points on the sample in less than one hour. The X-ray counts were normalized to silica and the surfaces of different samples and were compared for the presence and the distribution of different elements. Images and frequency curves were obtained to show the distribution of elements on the sample surface.

[Myung, 2008] measured heavy metal concentrations in soils and plants in and around a copper-tungsten mine in southeast Korea. They studied the influence of past base metal mining on the surface environment. The metal concentrations in plant species generally decreased in the following order: spring onions > soybean leaves > perilla leaves≈ red pepper > corn grains≈ jujube grains. This pattern varied moderately between different elements. The factors that influence the bioavailability of metals and their occurrences in crops include pH, cation exchange capacity, organic matter content, soil texture, and interactions of the target elements. They concluded that the accumulative metal concentrations in soils are the main controllers of their content in plants.

[Abu-Rukah, 2000] studied the chemical speciation for 15 elements at depths of 10-cm intervals in 6 cores at two locations along the Yarmouk River. The heavy-metal enrichment factors (EFs) and anthropogenic factors (AFs) showed that Cd and Ni for all the cores, and Mn, Zn, Cr, Co and Pb for core 3 at location A are anthropogenically enriched. The results show that the sediments of the Yarmouk River are not contaminated with Fe, Cr, and Mn; not to moderately contaminated with Ni, Co, and Zn; moderately contaminated with Pb; and strongly to extremely contaminated with Cd.

2 Sampling and Characterization

2.1 Sampling

2.1.1 Study Region

Soils samples were collected from three different regions in Palestine in December 2015 for a series of measurements and analyses using a number technique. The samples were taken from Hebron south of west bank, Qalqilia north, and Jericho in the middle and near the dead sea. A total number of 36 samples were collected, 12 from each region and taken at 4 depths (10, 20, 30, 40 cm) from 3 locations within 1 km^2 area. Figure 2.1, 2.2 and 2.3 show sites maps.

The data was taken from the Arroub valley near Hebron, Qalqilia internal plain and Jericho Jordan valley plain. The three locations are agricultural lands that lay on top of major water basins, and could potentially be high risk regions with variable exposure to pollutants and sewage. In the study we compared the three areas in correlation with their histories.

Figure 2.1: Image from google earth for places of taking Hebron samples.

Figure 2.2: Image from google earth for places of taking Jericho samples.

Heavy metals found in sewage constitute a major source of soil pollution. These heavy metals remain for long time and leave negative effects for many years and perhaps for few generations to come. They represent adverse effects on the environment and high risks on the underground water located in these regions.

Figure 2.3: Image from google earth for places of taking Qalqilia samples.

We seek through this study to improve agricultural productivity and rid crops of pests and sanitation, which are disposed randomly in the region because of the lack of sewage systems hence the importance of the study for the community.

2.1.2 Sampling Method

The Sampling method is outlined in the following:

1. For each region samples were taken from 3 places located within an area of 1 km^2.
2. For each place 4 samples were taken at 4 depths, namely at 10, 20, 30, 40 cm. A total of 12 samples from each region were collected.
3. Samples were collected in the testing tray. The label is composed of 5 digits' **ab-c-de**, with **ab** standing for the first 2 letters of the region name; **c** stands for the place number, and **de** stand for the depth in cm. example: He-1-10cm: The sample from Hebron, first place, at a depth of 10cm.

Table 2.1: Contains all 36 samples and describes all tests made on each sample.

Sample	Description	Tests taken
Jericho		
Je-1-10cm	Jericho site 1 depth 10 cm.	ICP-MS; XANES; EXAFS
Je-1-20cm	Jericho site 1 depth 20 cm.	pH; ICP-MS; SMC; SVOC; XANES; EXAFS
Je-1-30cm	Jericho site 1 depth 30 cm.	ICP-MS ; XANES; EXAFS
Je-1-40cm	Jericho site 1 depth 40 cm.	ICP-MS; XANES; EXAFS
Je-2-10cm	Jericho site 2 depth 10 cm.	ICP-MS; XANES; EXAFS
Je-2-20cm	Jericho site 2 depth 20 cm.	pH; SMC; SVOC
Je-2-30cm	Jericho site 2 depth 30 cm	
Je-2-40cm	Jericho site 2 depth 40 cm	
Je-3-10cm	Jericho site 3 depth 10 cm	ICP-MS; XANES; EXAFS
Je-3-20cm	Jericho site 3 depth 20 cm	pH; SMC; SVOC
Je-3-30cm	Jericho site 3 depth 30 cm	
Je-3-40cm	Jericho site 3 depth 40 cm	ICP-MS
Hebron		
He_1_10cm	Hebron site 1 depth 10 cm	ICP-MS; XANES; EXAFS
He_1_20cm	Hebron site 1 depth 20 cm	pH; ICP-MS; SMC; SVOC XANES; EXAFS
He_1_30cm	Hebron site 1 depth 30 cm	ICP-MS; XANES; EXAFS
He_1_40cm	Hebron site 1 depth 40 cm	ICP-MS; XANES; EXAFS
He_2_10cm	Hebron site 2 depth 10 cm	ICP-MS; XANES; EXAFS
He_2_20cm	Hebron site 2 depth 20 cm	pH; SMC; SVOC
He_2_30cm	Hebron site 2 depth 30 cm	
He_2_40cm	Hebron site 2 depth 40 cm	
He_3_10cm	Hebron site 3 depth 10 cm	ICP-MS; XANES; EXAFS
He_3_20cm	Hebron site 3 depth 20 cm	pH; SMC; SVOC
He_3_30cm	Hebron site 3 depth 30 cm	

He_3_40cm	Hebron site 3 depth 40 cm	ICP-MS
Qalqilia		
Qal_1_10cm	Qalqilia site 1 depth 10 cm	ICP-MS ; XANES; EXAFS
Qal_1_20cm	Qalqilia site 1 depth 20 cm	pH; ICP-MS; SMC; SVOC XANES; EXAFS
Qal_1_30cm	Qalqilia site 1 depth 30 cm	ICP-MS; XANES; EXAFS
Qal_1_40cm	Qalqilia site 1 depth 40 cm	ICP-MS ; XANES; EXAFS
Qal_2_10cm	Qalqilia site 2 depth 10 cm	ICP-MS; XANES; EXAFS
Qal_2_20cm	Qalqilia site 2 depth 20 cm	pH; SMC; SVOC
Qal_2_30cm	Qalqilia site 2 depth 30 cm	
Qal_2_40cm	Qalqilia site 2 depth 40 cm	
Qal_3_10cm	Qalqilia site 3 depth 10 cm	ICP-MS; XANES; EXAFS
Qal_3_20cm	Qalqilia site 3 depth 20 cm	pH; SMC; SVOC
Qal_3_30cm	Qalqilia site 3 depth 30 cm	
Qal_3_40cm	Qalqilia site 3 depth 40 cm	ICP-MS

2.2 Samples Characterizations

2.2.1 Soils Moisture Contents (SMC)

Generalities

Soil moisture content (SMC) is defined as the ratio of water to solids masses present in the sample. SMC is a soil variable parameter, and its value depends on many factors including time, location, weather, climate, geography, soil constituent, heterogeneity of the soil, geological soil formations, soil biological compositions, and the farming fields in an area. Many methods for measuring a SMC in a soil can be used like, volumetric water content, gravimetric water content, degree of soil saturation, geophysical soil moisture sensors and satellite remote sensing **[cfr.washington.edu]**. The SMC is useful in many life applications such as, hydrology, forestry, soil mechanics engineering, earth and agricultural sciences, and in measuring the groundwater aquifer capacity. We used the gravimetric water Concentration (SMC) method to measure the SMC for nine samples covering the three places in each region. [http://www.cfr.washington.edu/classes.esrm.410/moisture.htm]

Measuring SMC

Nine empty porcelain dishes were washed, dried and weighted. Fifty grams of none treated material were taken form each sample. To avoid mass loss during preparation, the samples with the dry dishes were weighted again. Then the samples were dried in an oven at 105 ℃ for 24 hours. The dry samples their weights were measured for a final step. The moisture contents ratio was calculated as

SMC = $(\frac{M_{W-}M_D}{M_D})$ * 100% where M_W : the weight of the wet sample and the dry dish at room temperature. M_D: the weight of the dried sample and dry dish at 105 ℃. SMC measurements for the three regions are shown in Figure 2.4.

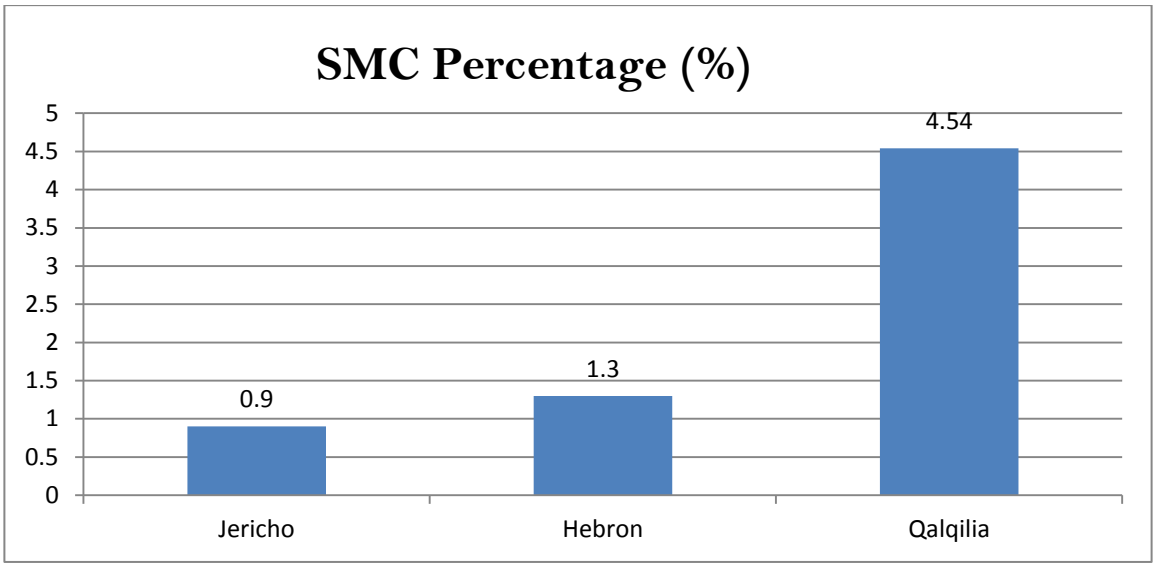

Figure 2.4: Moisture contents in soils from Jericho, Hebron and Qalqilia.

The highest SMC content was observed in Qalqilia soil (~4.54 %). The SMC variation is due to different soils types and climate. Jericho has a loam soil type with a hot environment, which tends to by dry with a minimum moisture contents; Hebron, has a slight increase due to a moderate temperature. Qalqilia plain soil is clay and characterized by high moisture content in addition to the humid weather in the internal plains not too far from the sea.

2.2.2 Soils pH

Generalities

pH is the symbol for the logarithm of the reciprocate of Hydrogen Ions in mole per liter. It is defined as the degree of acidity or basicity (alkalinity) of a sample. pH can be used to describe the acidity or alkalinity of a chemical solution on a scale of 0 (hypo acidic) to 14 (hyper alkaline). The pH value is defined as the negative base 10 logarithm of the activity of hydronium ion (H_3O^+) in the solution or pH = -$Log_{10}[H_3O^+]$ where $[H_3O^+]$: the molar concentration of Hydronium ion in a solution.

The pH values range is 0-14, where 7 represents neutral medium, less than 7 is acidic and more than 7 is basic medium. For a soil the optimum pH range for most plants is between 5.5 and 7 **[**Perry, Leonard**]**. However, many plants can adapt to pH values out of this range. Table 2.2 shows the soil pH classifications of soils types.
[http://www.nrcs.usda.gov/wps/portal/nrcs/detail/soils/ref/?cid=nrcs142p2_054223]

Table 2.2: Soils pH classifications.

Reaction Class	Range in pH
Ultra-acidic	1.8-3.4
Extremely acidic	3.5-4.4
Very strongly acidic	4.5-5.0
Strongly acidic	5.1-5.5
Moderately acidic	5.6-6.0
Slightly acid	6.1-6.5
Neutral	6.6-7.3
Slightly alkaline	7.4-7.8
Moderately alkaline	7.9-8.4
Strongly alkaline	8.5-9.0
Very strongly alkaline	9.1-11.0

Measuring the soil pH is important to determine the chemical forms of a supplied nutrients for the plants. In addition, pH affects the plant growth, micro-organisms bioavailability, soil nutrient uptake and availability, and the soil structure. The different pH values result from the soil chemical and biological constituents and other components, like minerals, salts and air content of CO2 [Leonard Perry,2003].

Measuring pH in Soil Samples

Nine dried and grinded soil samples (12.5 grams each) from three regions at depth 20 cm were subject to pH measurements. Each sample was dissolved in 50 mL of distilled water. The solutions were stirred for one minute, and left to settle down for couple of minutes.

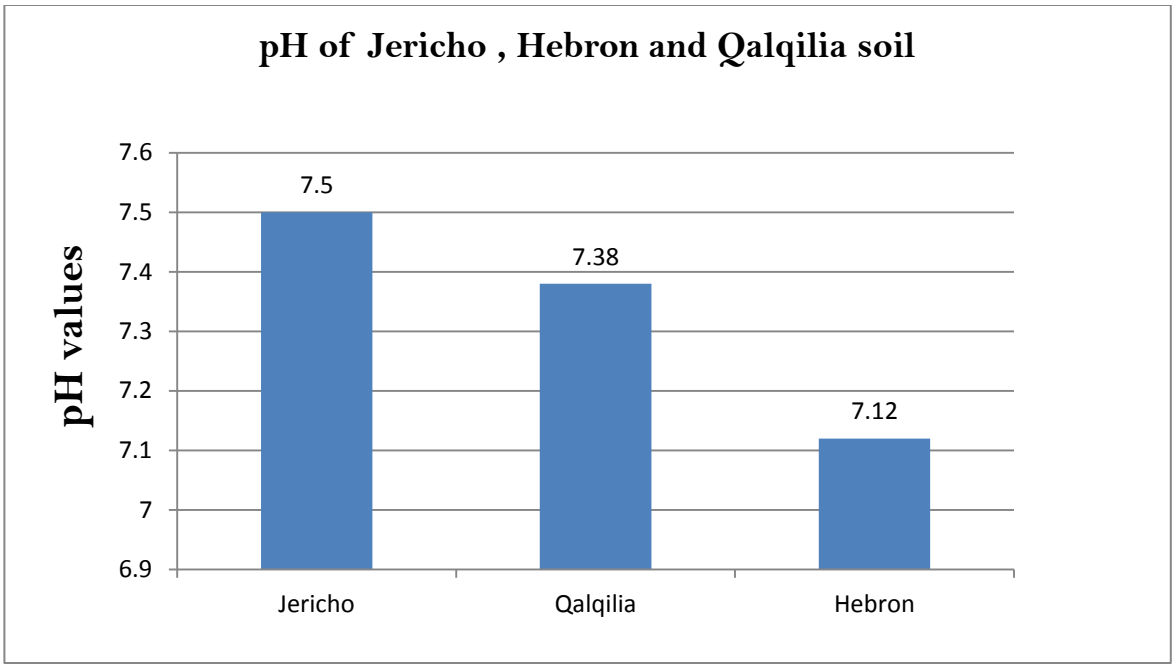

Figure 2.5: Jericho, Hebron and Qalqilia soils pH results.

This was followed by stirring each solution for 10 minutes three times, then rested for 30 minutes then the solution was stirred again for the last time. Afterward we inserted the electrodes of the pH meter in the solution at a depth of 3 cm from the surface. Readings were taken after 30 seconds. Figure 2.5 shows the pH results. Most heavy metals mobility and availability depend on the soil pH and they are highest in acidic soils compared to neutral and alkaline soils. Jericho soil has high pH 7.5, Qalqilia 7.38 and Hebron soil pH 7.12. All pH values are within the neutral soil with slightly alkaline inclinations.

2.2.3 Soils Volatile Organic Contents (SVOC)

Generalities

SVOC measures the volatile organic components found in a soil. The functional definition of soil organic matter excludes organic materials larger than 2 mm in size [Brian Murphy, 2008]. The volatile organic matter can be classified in three categories: i) small fresh residues of plant and living organisms, ii) active decomposed organic matter and iii) stable organic matter. The SVOC consists of living organic matter, plant and animal residues, remains of root and plant materials, cells and tissues of soil organisms, material being synthesized of living organisms in a soil, dissolved and particulate organic matter, humus soil and inert or highly

carbonized matter. Table 2.3 shows the percentage of major soil organic matter components. [Soil Quality Institute,1999]. SVOC normal values range from 1% to 6% of the total topsoil mass for most upland soils. Soils with upper horizons of less than 1% organic matter are mostly limited to deserts while SVOC in low-lying lands can reach 90%. Soils with 12-18% SVOC are generally classified as organic soils [Wikipedia].

Table 2.3: Major soil organic matter components percentage in atypical soil.

Soil Organic Matter Component Name	Percentage (%)
Living organisms	< 5%
Fresh organic residue	< 10%
Humus soil	33% - 50%
Decomposing organic matter	33% - 50%

Factors affecting SOC include climate conditions, rainfall, temperature, moisture, soil aeration and soil texture. Regarding the speed of SOC decomposition in a soil, the warmer and humid is the climate, the faster the SOC is decomposing and vice versa. Additionally, the higher is the oxygen level in a soil, the higher the SOC decomposes and vice versa.

Measuring SVOC

The previously used samples for moisture content experiments are reused for the SVOC measurements. Dry soils samples were reheated and burned with dry dishes at 500 ℃ for 24 hours, then reweighed.

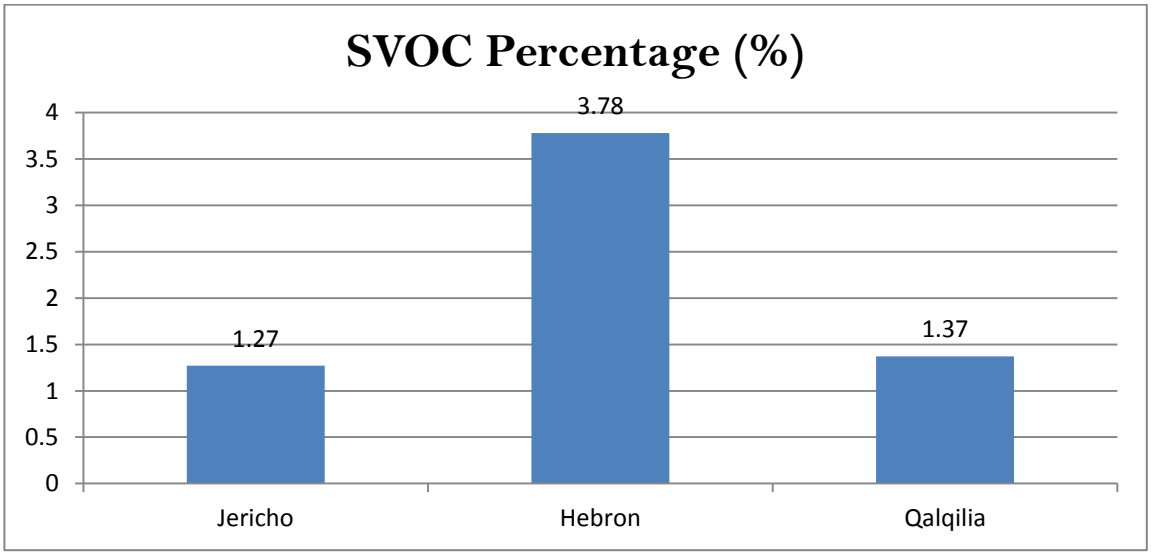

Figure 2.6: Jericho, Hebron and Qalqilia soils organic contents percentages values.

The SVOC was calculated using SVOC = $\left(\frac{M_{D-M_B}}{M_B}\right) * 100\%$ where M_D: total weight of dried sample at 105 ℃,; M_B: total weight of burned sample at 500 ℃. The SVOC measurements of three regions are shown in the Figure 2.6. The high SVOC values for Hebron sites indicate the soil is more clay compared to Jericho Loamier soil. Hence Jericho soil is expected to have higher concentration of heavy Elements such as Cr, Cu, Zn, Ni. ICP-MS measurements confirmed these expectations.

2.3 Inductively Coupled Plasma-Mass Spectroscopy (ICP-MS)

2.3.1 Generalities

The ICP-MS is used to measure very low concentrations of trace elements, sometimes in parts per trillion (ppt). This technique is 30 to 35 years old and can be considered as new and sophisticated technique in analyzing trace elements and it is the fastest growing technique for trace elements concentrations measurements.
[https://crustal.usgs.gov/laboratories/icpms/intro.html]

ICP-MS, is important in analyzing chemical elements because the detection limit is lower than 1 ppb (part per billion) for many elements; an isotopic analysis can be achieved; and because of reproducibility of the measurements. Figure 2.7 shows by the ICP-MS technique and their detection limits for some very rare elements. [http://crustal.usgs.gov].

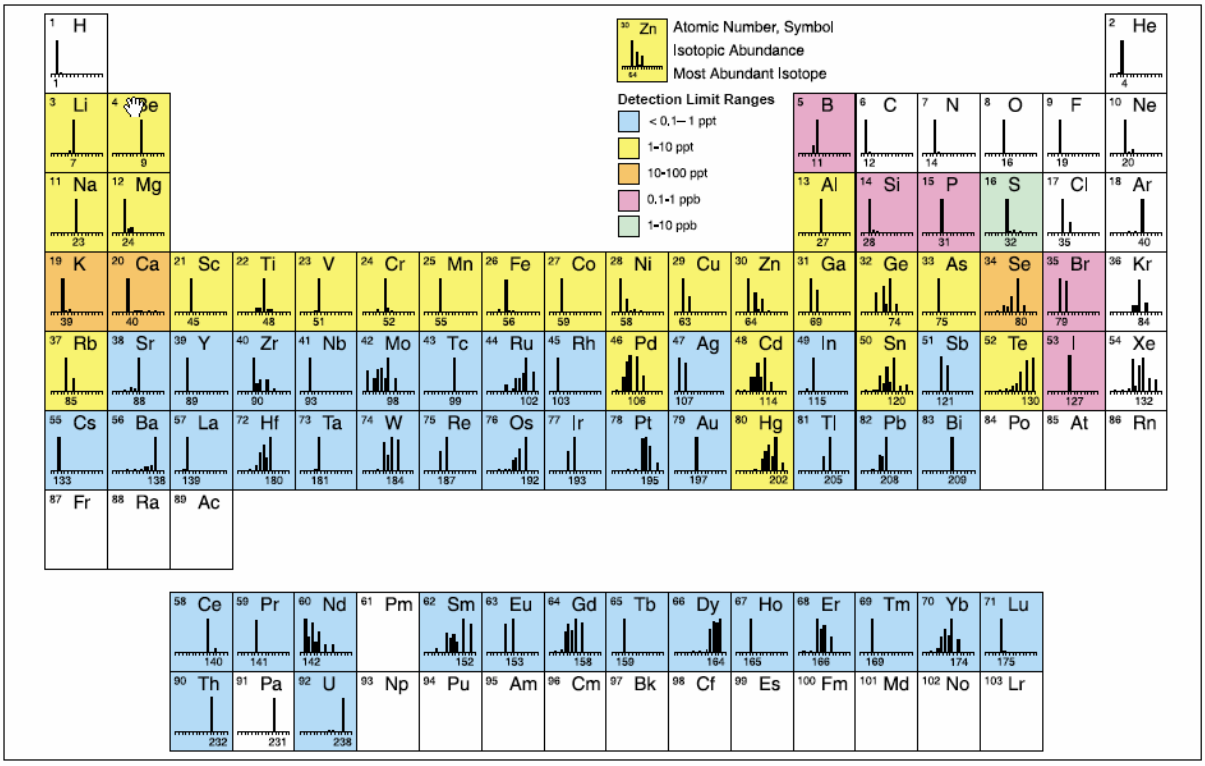

Figure 2.7: ICP -Mass Spectroscopy detectable elements and their detection limits.

2.3.2 ICP-MS Technique

Figure 2.8 shows the ICP-MS setup and principal components. [http://biochem.pepperdine.edu]. First we mixed the samples enough to make them homogeneous, then took about 0.25 g from each sample with a total of 21 samples . They were placed in separate tubes each containing 3 ml of 65% Nitric Acid (HNO_3); 2 ml of 48% Hydrofluoric Acid (HF); and 2 ml of (H_2O_2). The samples were put in warm water bath at 70 ℃ overnight. The Measurements were done at the JAEC in Jordan using the ICP-MS model (820-MS).

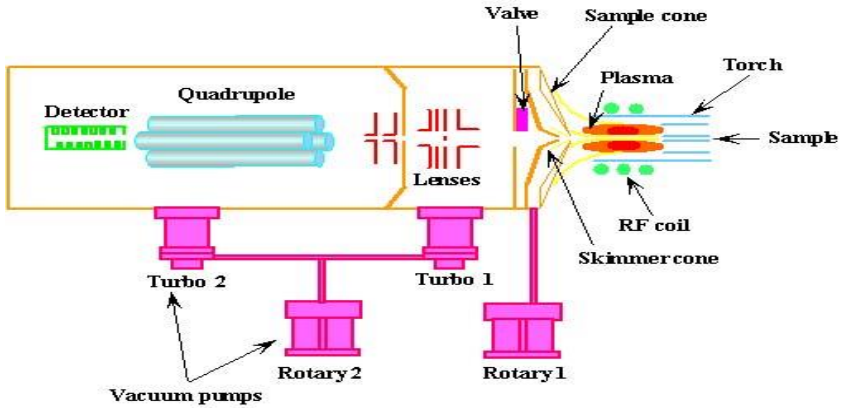

Figure 2.8: A schematic diagram of ICP-MS experiemental setup.

2.3.3 ICP-MS Measurements

The main purpose of this study is to compare metal contents of soils in Hebron, Jericho and Qalqilia irrigation sites respectively, with the maximum permissible levels set by World Health Organization (WHO). The results are expected to create awareness among the public on the safety of consuming vegetables grown in such areas.

Table 2.4: Maximum allowed limits of heavy metals in soils (ppm) set by World Health Organization.

Chemical Element	Maximum permissible level in soil (ppm)
Cd	3
Co	50
Cr	100
Cu	100
Mn	2000
Ni	50
Pb	100
Zn	300

The results obtained by ICP-MS in part per million(ppm). The maximum allowable limits standards for heavy metals in soils have been established by regulatory bodies such as World Health Organization (WHO), Food and Agricultural Organization (FAO) and Ewers U, Standard Guidelines in Europe.

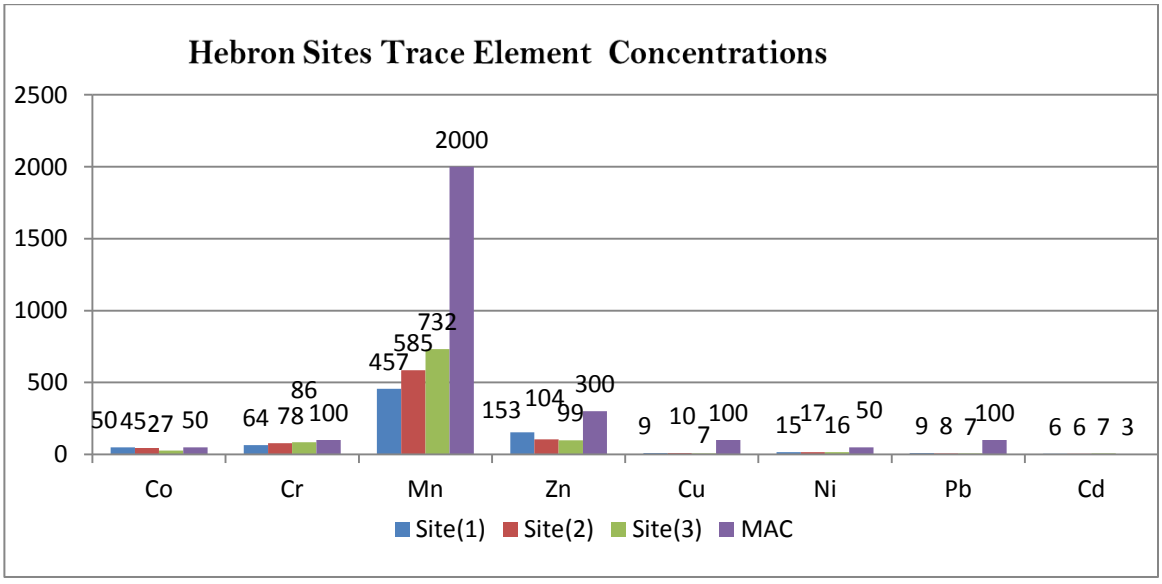

Figure 2.9: Hebron sites (1,2,3) trace elements concentrations by ICP-Ms techniques with the Maximum Allowable Concentrations (MAC) elements in a soil at 10 cm depth.

as shown in Table 2.4 [Chiroma, 2014]. Figure 2.9 shows the concentrations of Co, Cr, Ni, Pb, Cd, Zn, Mn and Cu in Hebron soil at depth of 10 cm of three sites (1, 2, 3). Figure 2.10

illustrates the concentrations of Co, Cr, Ni, Pb, Cd, Zn, Mn and Cu in Jericho soil at depth of 10 cm of three sites (1,2,3).

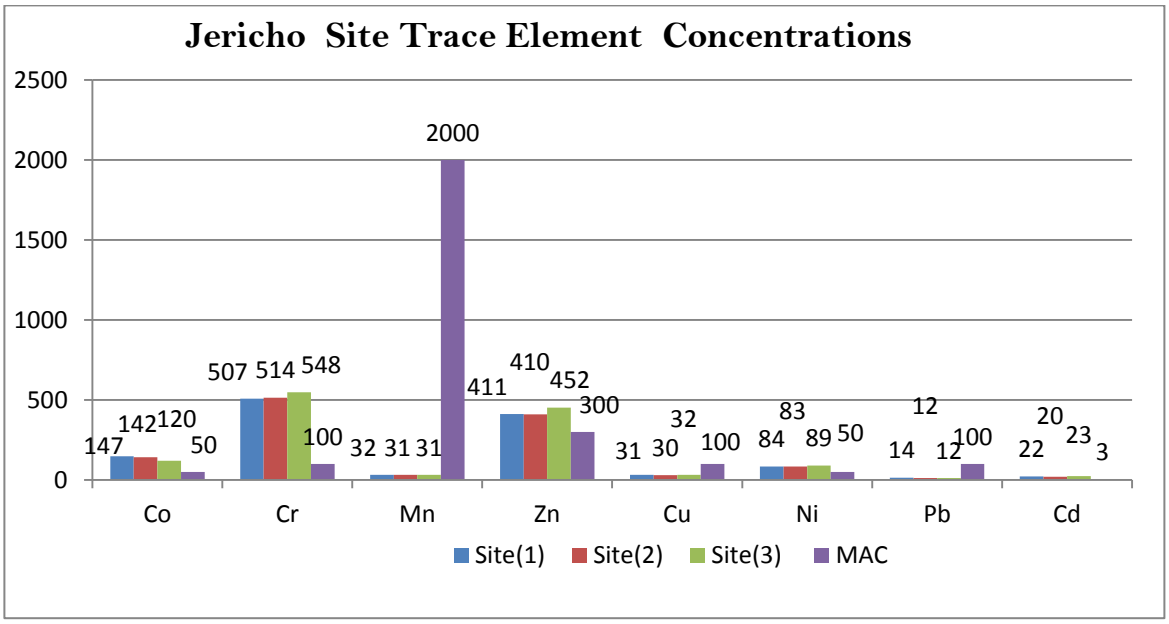

Figure 2.10: Jericho sites (1,2,3) trace elements concentrations by inductively ICP-Ms techniques with the Maximum Allowable Concentrations (MAC) elements in a soil at 10cm depth.

Figure 2.11 shows the concentrations of Co, Cr, Ni, Pb, Cd, Zn, Mn and Cu in Qalqilia soil at depth of 10 cm for the three sites.

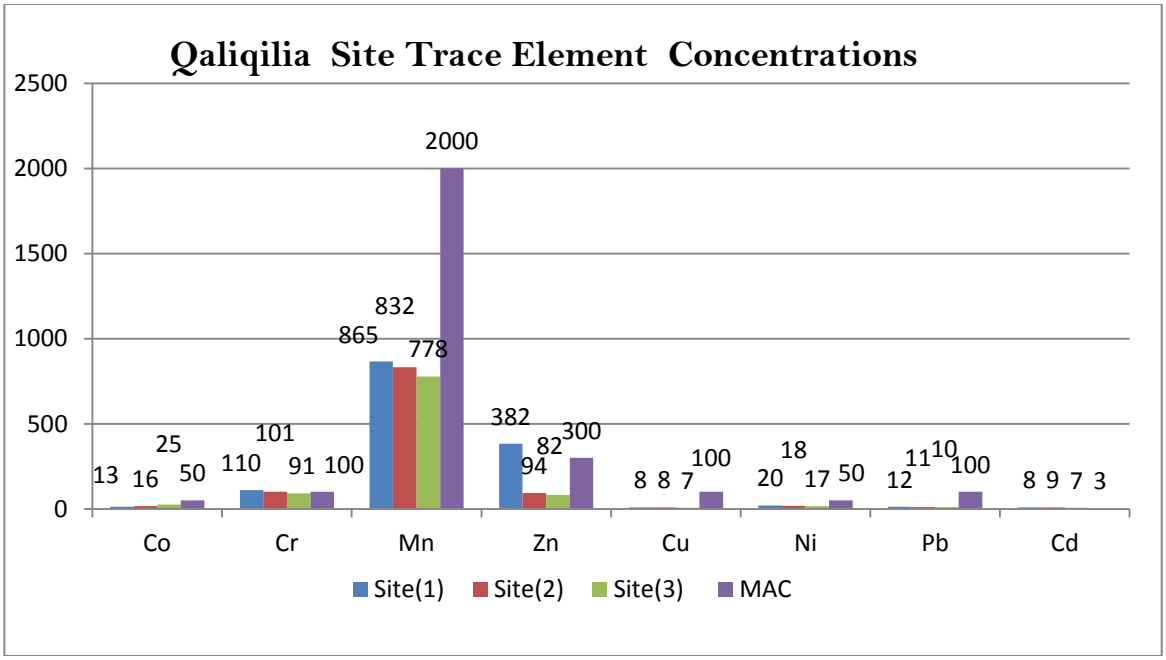

Figure 2.11: Qalqilia sites (1, 2, 3) trace elements concentrations by ICP-Ms techniques with the maximum allowable concentrations elements in a soil at 10 cm depth.

Comparing heavy metals concentrations between Jericho, Hebron and Qalqilia

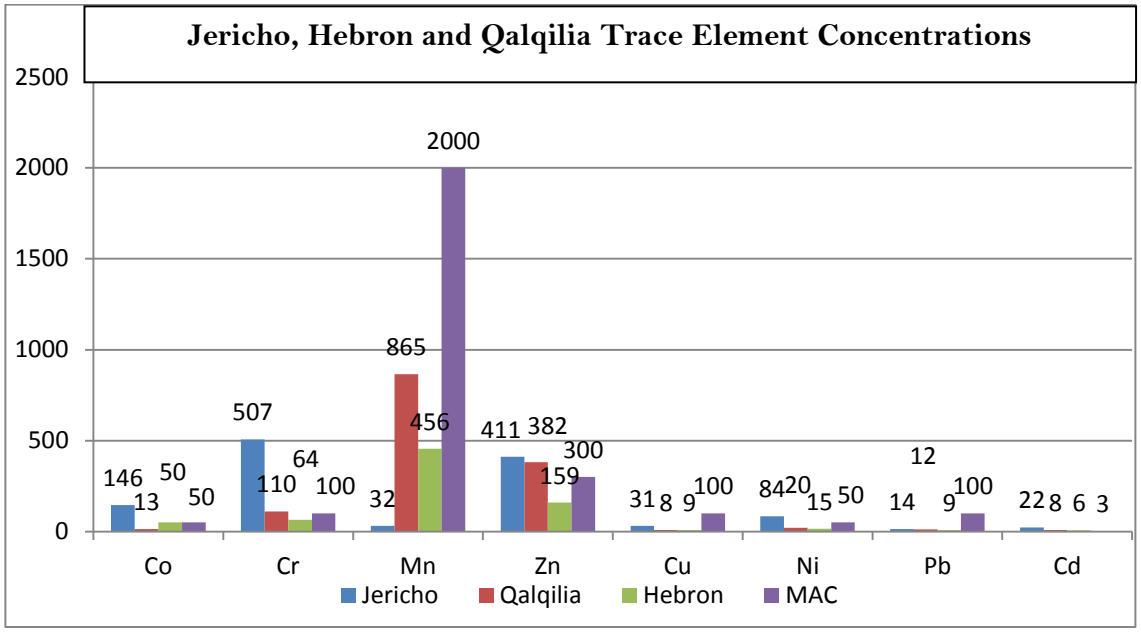

Figure 2.12: A comparison between Jericho, Hebron and Qalqilia trace elements concentrations by ICP-Ms techniques, with the Maximum Allowable Concentrations (MAC).

2.3.4 ICP-MS measurements and Observations

Cobalt Determination: Jericho Soils have the highest contents (146 ppm) of Co, while the Qalqilia Soils have the least concentration (12 ppm). Among the Hebron Soils Co concentration, occurred in the range of (27–50 ppm) below WHO limit (50 ppm). In Jericho Soils Co concentration occurred in the range of (120-147 ppm) above WHO limit, While the Qalqilia Soils Co concentration occurred in the range 13-25ppm well below WHO limit.

Chromium Determination: The Soils Cr contents were found in the range 64-548 ppm. The highest and lowest contents of Cr occurred in Jericho and Hebron Soils respectively. In Hebron, the Cr concentration occurred in the range of 64-87 ppm well below WHO's limit (100 ppm). In Qalqilia Soils Cr concentration occurred between 91-110 ppm. Jericho Solis Cr concentration are in the range 351-548 ppm.

Zinc Determination: The Jericho Soils have the highest Zn contents (433 ppm), while Hebron Soils have the least (76 ppm). Among the Hebron trace Zn concentration, occurred in the range of 76–151 ppm below WHO limit (300 ppm). In Jericho soil, concentration of Zn occurred in the range of 273-433 ppm which is above WHO limits, while the Qalqilia trace concentration of Zinc occurred between 82-381 ppm above WHO limit for some cases.

Manganese Determination: It is a very essential trace heavy metal for plants and animal's growth. Its deficiency produces severe skeletal and reproductive abnormalities in mammals. High concentration of Mn causes hazardous effects on lungs and brains of humans. Qalqilia Soils contained the highest levels (766-864 ppm) of Mn, while Jericho Soils contained the least level (21-32 ppm). In Hebron Soils Mn contents varied in the range of 456-741 ppm. While in Jericho trace had least with the range between 21-32 ppm. WHO's permissible Mn limit in soil is 800 ppm.

Nickel Determination: It is also an essential element for plants and animals. In small quantity, nickel is necessary for the regulation of lipid contents in tissues and for the formation of red blood cells. But at high levels, it becomes toxic and causes severe diseases like loss of body weight, loss of vision, and heart and liver failures, as well as skin irritation. Experimental data revealed that Ni concentration in soil samples occur in the range of 15-89 ppm. Jericho Soils have the highest levels between 70-89 ppm, Hebron Soil have contents between 15-19 ppm. Qalqilia Soils Ni concentration was found in the range of 17–21 ppm. WHO's permissible Ni limit in soils is 50 ppm.

Copper Determination: Being an essential trace element, it is necessary for many enzymes. It is needed for the normal growth and development. High concentration of Cu causes metal fumes fever, hair and skin de-colorations, dermatitis, respiratory tract diseases, and some other fatal diseases in human beings. The highest Cu level were found in Jericho Soils in the range 70-89 ppm, and the soil of Hebron Soils have Cu in the range 6.3-9.1 ppm. Qalqilia Solis Cu concentration are in the range of 6.7-8.2 ppm. WHO's permissible Copper limit of in soil 100 ppm.

Lead Determination*:* It is a non-essential heavy metal. Pb causes oxidative stress and contributes to the pathogenesis of lead poisoning by disrupting the delicate antioxidant balance of the mammalian cells. High level accumulation of Pb in body causes anemia, colic, headache, brain damage, and central nervous system disorder. The soil samples contained the Pb concentration in a range of 0.02–89 ppm. Jericho Soils have the highest levels in the range 78-89 ppm of Pb, while the soil of Hebron Soils range is 0.02-19 ppm. Qalqilia Soils Pb concentration varied in the range of 10-12.5 ppm. WHO's permissible lead limit in soil is 100 ppm.

Cadmium Determination*:* It is also a non-essential heavy metal. It is extremely toxic even at low concentration. It causes learning disabilities and hyperactivity in children. Cd normal concentrations in soils is in the range of 19 and 23 ppm. The Jericho Soils levels are 19-23 ppm, while the Hebron Soils have contents in the range 3-6.6 ppm. Qalqilia Solis Cd concentration varied in the range of 6.5-8.5 ppm, WHO cadmium limit in soil is 3.5 ppm.

2.3.5 (ICP-MS) Measurements Summary

Jericho Soils have the highest concentrations of Co, Cr, Cu, Ni, Pb, Zn and Cd except Mn. Co, Cr, Zn, Cd, Ni concentrations are above WHO's recommended level. Hebron concentrations are within WHO limits except Cd (6.5 ppm). Most Qalqilia concentrations are within WHO's limits except few cases with Cd, Zn and Cr.

Part II

Structural Analysis

3

Background and Experimental Setup

3.1 X-ray Absorption Fine Structure (XAFS)

X-ray Absorption Fine Structure (XAFS) spectroscopy provides information about the electronic and structural properties of catalysts under reaction conditions and in the presence of reactants. XAFS is a powerful method for probing local coordination environment of metals and other elements in a variety of samples. It utilizes photons exclusively (i.e., photons in and using transmission or fluorescence yield photons out). It is a short-rang order method that can be used regardless of physical state of sample, and requires little sample preparation, with the possibility of using it as a direct probe. It has become a popular method of investigation in the environmental community because samples are often complex chemical mixtures of various species containing multiple elements.

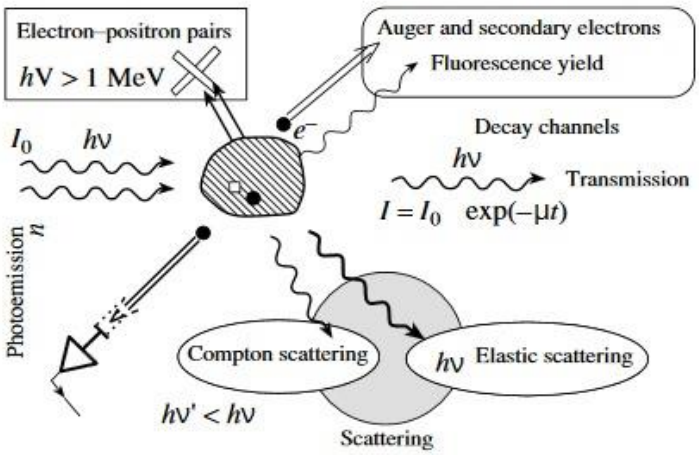

Figure 3.1: X-Rays interaction with a substance

XAFS refers to the details of how x-rays are absorbed by atoms at energies near and above their core-level binding energies. It is the modulation of an atom x-ray absorption probability due to the chemical and physical state of the atom. XAFS spectra are especially sensitive to the formal oxidation state, interatomic distances, coordination number and species of the at-

oms immediately surrounding the selected element. Because of this dependence, XAFS provides a practical, and relatively simple, way to determine the chemical state and local atomic structure for a selected atomic species [Mathew Neville, 2004]. It is commonly divided into two main regions, XANES and EXAFS. Figure 3.1 shows the elementary interaction of x-rays with matter.

3.2 X-ray Absorption Near Edge Structure (XANES)

The excitation of an atom by an X-ray source, changes the electron configuration , An absorption edge happens, due to the scanning of the binding energy by an X-ray source, so an instance absorption appears by some characteristic core electrons. "A core hole is the space a core electron occupied before it is removed by an absorbed an X-ray photon. Core holes are extremely energetic (electronegative) which leads to their unstable nature. Core holes are created through either a core electron absorbing an X-ray photon (X-ray absorption) or part of the photon's kinetic energy (X-ray Raman scattering). [http://chemwiki.ucdavis.edu].

A schematic of XANES single scattering of an exited atom is shown in Figure 3.2, Moreover, all the absorptions edges for all elements in the periodic table is being presented in the following table 3.1 [http://chemwiki.ucdavis.edu].

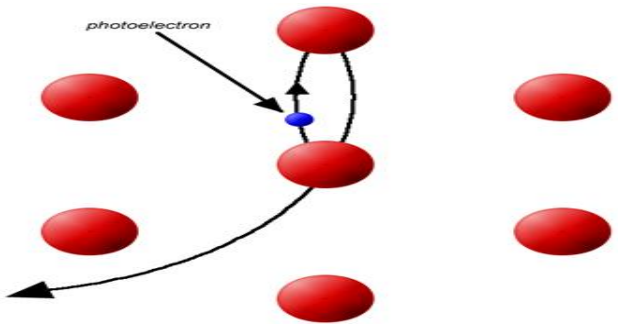

Figure 3.2: Exited atom single scattering

Table 3.1: Elements atoms Absorption Edges.

K edge	1s			
Ledge	2s	2p		
M edge	3s	3p	3d	
N edge	4s	4p	4d	4f

3.2.1 XANES Experiments

We used the samples in the form of fine powder. It was prepared as soils pallets by weighing 1 gm of the selected samples to be tested by XANES technique. Then we grinded the samples as much as we can, to make them very fine, under high pressure up to 5 bar. After that we added Polyvinylpyrrolidon (PVP) powder to the soils samples, to make them compacted samples. The last step is to run the experiments for several hours for each sample. XAFS data were collected by changing the photons energy and collect the number of photons before and after the sample. In our study we analyzed the samples using Athena software, for the XANES analyzing technique. Figure 3.3 shows XANES and EXAFS regions and the edge step in XAFS analytical data for Iron(II) Oxide (FeO). Figure 3.4 shows a schematic of an XAFS experiment [http://cnx.org]

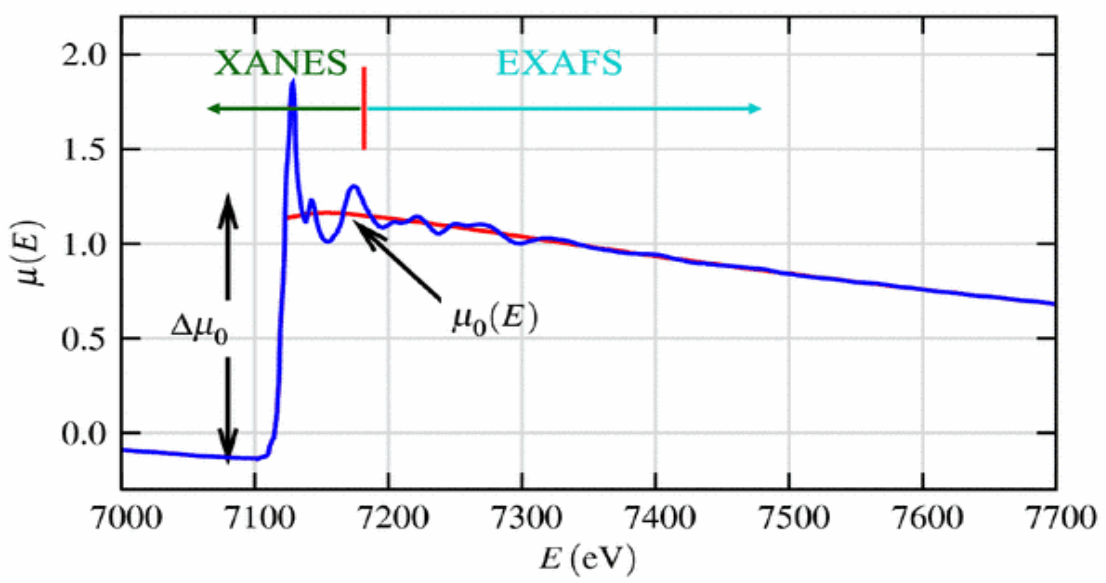

Figure 3.3: XAFS spectra of Iron(II)Oxide

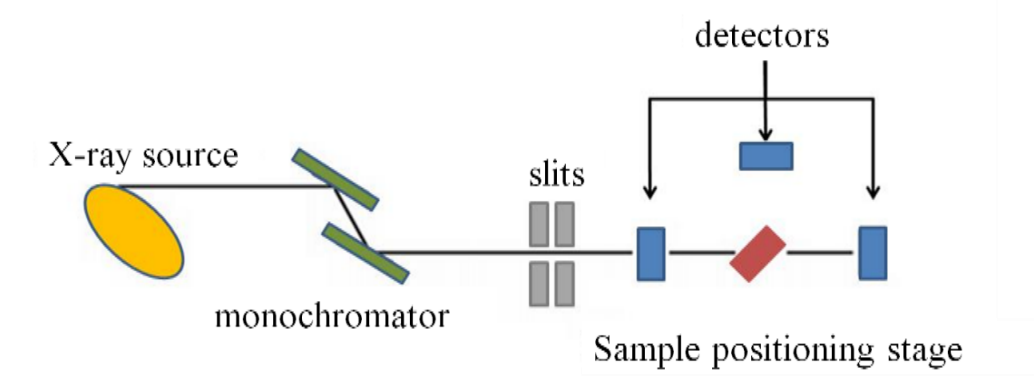

Figure 2.4: Schematic diagram of the basic components of XAFS beamline experiment

3.3 Extended X-ray Absorption Fine Structure (EXAFS)

XANES region extends for 50-100 eV beyond an absorption edge and is determined by the local density of vacant states in an absorbing atom, and by multiple-scattering effects such as scattering of an excited photoelectron on several atoms [GAUR et al., 2013]. The EXAFS region beyond is dominated by single scattering and extends up to 400-1000 eV from an edge. Its upper bound is determined by the signal-to-noise ratio and/or another absorption edge [Aksenov, 2001] , Figure 3.5, Schematic view of photoelectron scattering on neighbor atoms, determining the EXAFS oscillations . [http://www.ung.si/~arcon/xas/xanes/xanes.htm].

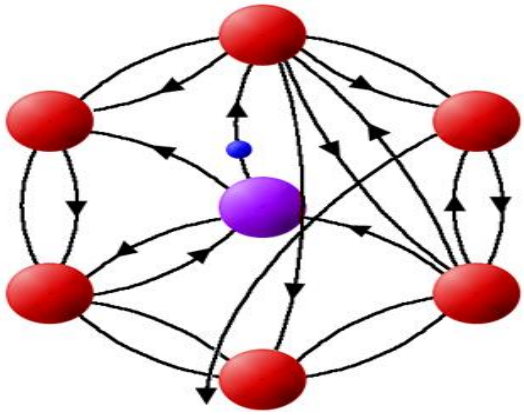

Figure 3.5: Exited atom multiple scattering

The EXAFS is observed when the X-ray energy exceeds the shell ionization energy. We can relate this occurrence to the X-ray absorption coefficient, which is the basis of EXAFS principle. The X-ray absorption coefficient, describes the relationship between the X-ray intensity of the incident and outgoing beams at a depth x within the sample.
[http://chemwiki.ucdavis.edu].

The absorption coefficient is given by $I = I_0 e^{-\mu x}$ where I is the intensity of photons transmitted across some distance x, I_0 = the incident intensity, μ the linear attenuation coefficient and x the distance traveled. The EXAFS equation is given by

$$x(K) = \sum_j \frac{N_j}{kR_{j^2}} * f_j(k) * e^{-2k^2} \sigma_j^2 \left[2kR_j + \delta_j(k)\right]$$

where, f(k) and δ (k) include the scattering properties the excited atom neighboring atoms, N is the number of neighboring atoms, R is the distance to the neighboring atom, and σ^2 is the disorder in the neighbor distance [Mathew Newville, 2004]. Same samples XANES samples

can be to record EXAFS data. Several spectra are collected and averaged to reduce the signal to noise ratio. Each EXAFS scan is collected for about (1.5) hour. The data was processed using IFEFFIT and WinXAS software packages.

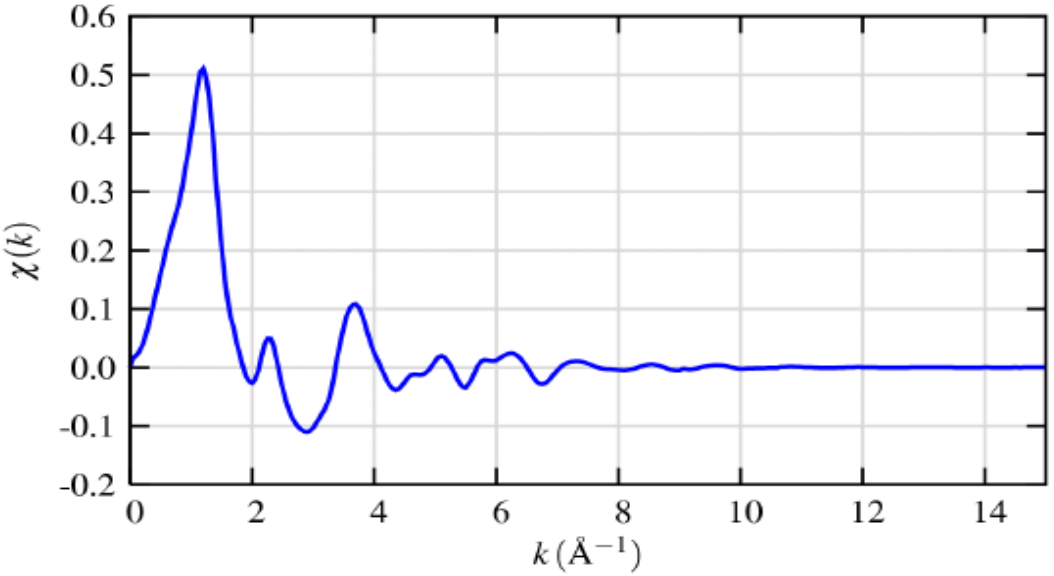

Figure 3.6: Isolated EXAFS (k) for FeO.

3.4 Experiments and Data Collection

3.4.1 Data Collection

XAFS data were collected at Cr (6002eV), Mn(6552ev) and Zn (9659 eV) K-edge using Beamline BL8 (XAS) at the Synchrotron Light Research Institute, in Thailand . The beamline operates at an energy range from 1.25 KeV- 10 KeV and delivering a photon flux of about 10^9 Ph/s.

In transmission, it is extremely important to have a homogeneous sample with no pinholes of optimized and constant thickness It is also important that the size of the particles needs to be finely grounded and homogeneous. Solutions produce the best transmission samples. in the case of environmental samples, these conditions may rarely be encountered, especially in the case of sensitive samples where the speciation of an element can change upon exposure to air or drying[Guillaume Morin, 1999], on the other hand, Fluorescent measurements put very few restrictions on the state of the sample, in fluorescence mode, the most important criterion is that the concentration of elements be less than 10% and that appeared with us by ICP-MS Results, for this reason, XAFS data were collected in Fluorescence mode using a 13-elements

Ge detector, and 3 scans per sample (30 min per scan), in which one ion-chambers (filled with helium to a required amount)were employed for measuring the incident intensity (I_0) and intensity after fluorescent (I_f) were detected using a 13-elements Ge detector (I_1-I_{13}). Fluorescence data were dead-time corrected before calculating the absorbance given by I_f/I_o equation.

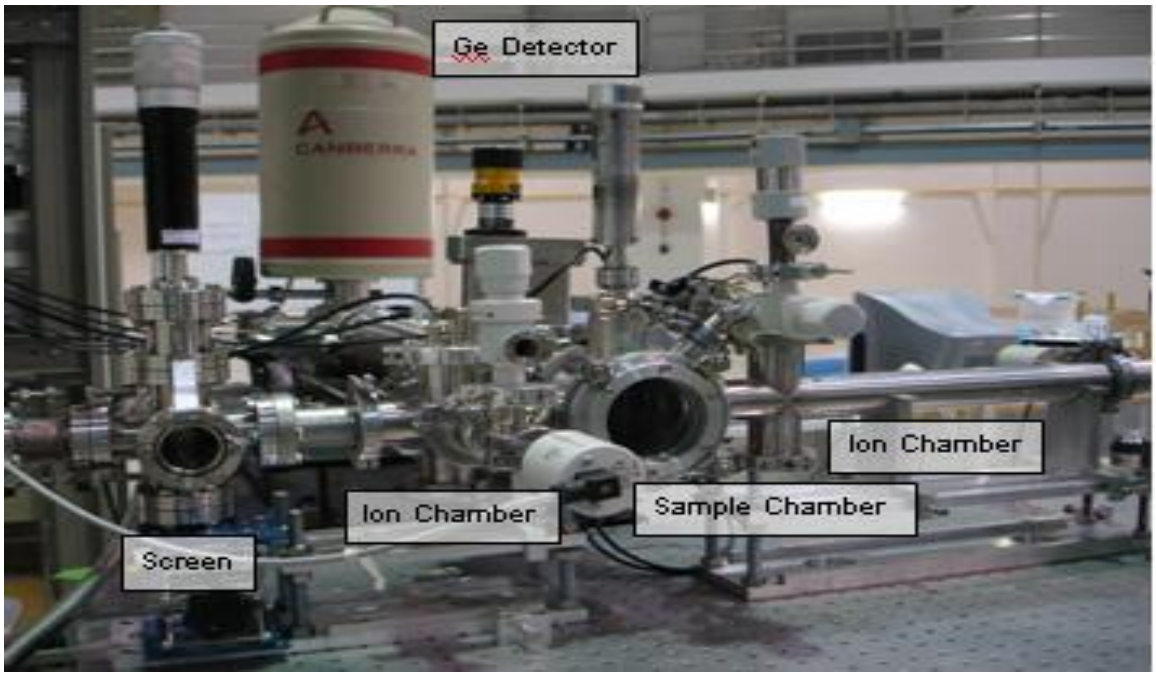

Figure 3.7: An XAS station.

The criterion for samples selection was to see the difference in the local environmental structure and bonding around Cr, Mn and Zn as a function of the depth, and from one site to another to reveal information about the soil systems.

Table 3.2: Samples tested by XAFS

Qalqilia	Hebron	Jericho
Qal_1_10cm	He_1_10cm	Je_1_10cm
Qal_1_20cm	He_1_20cm	Je_1_20cm
Qal_1_40cm	He_1_30cm	Je_1_30cm
Qal_2_10cm	He_1_40cm	Je_1_40cm
Qal_3_10cm	He_2_10cm	Je_2_10cm
	He_3_10cm	Je_3_10cm

3.4.2 Analysis Methods Used

XAFS data processing and analysis were performed using IFEFFIT software package following standard procedures **[**Ressler, 1998**],** for normalization and background subtraction. Using different experimental model compounds, linear combination fitting (LCF) analysis has been

performed to the X-ray Absorption Near-Edge Structure (XANES) data to estimate the concentration of different oxidation state species present in the samples. To determine the structure of various phases present in the system, detailed analysis of the EXAFS data was performed, after normalizing the Short-Extend XAFS spectra, EXAFS signals $\chi(k)$ were $k3$-weighted and Fourier Transformed (FT) using a Bessel window function.

Theoretical scattering paths, used for modeling experimental EXAFS, were calculated with FEFF [Rehr, 2000]. A multi-shell and a single scattering approximation were used for detailed analysis by curve fitting procedures, to reduce the number of free parameters, the amplitude reduction factor (S_0^2) was fixed at 0.9 based on initial fits. In addition, the shift in the threshold energy (ΔE) was linked for some the shells. Floating parameters of further shells were the coordination number (N), bond length (R) and the Debye–Waller factor (σ^2).

4

XANES and EXAFS Results and Discussions

4.1 Studying Chromium of Jericho Samples

4.1.1 XANES Data Analysis

09 K-edge (XANES) spectrums. The principal K-edge peak energy lies between 6002.69 and 6006.9 eV. To obtain quantitative chemistry information (formal oxidation state and geometry) for Cr, a linear combination fit analysis was carried out using the ATHENA software Figure 4.1b.

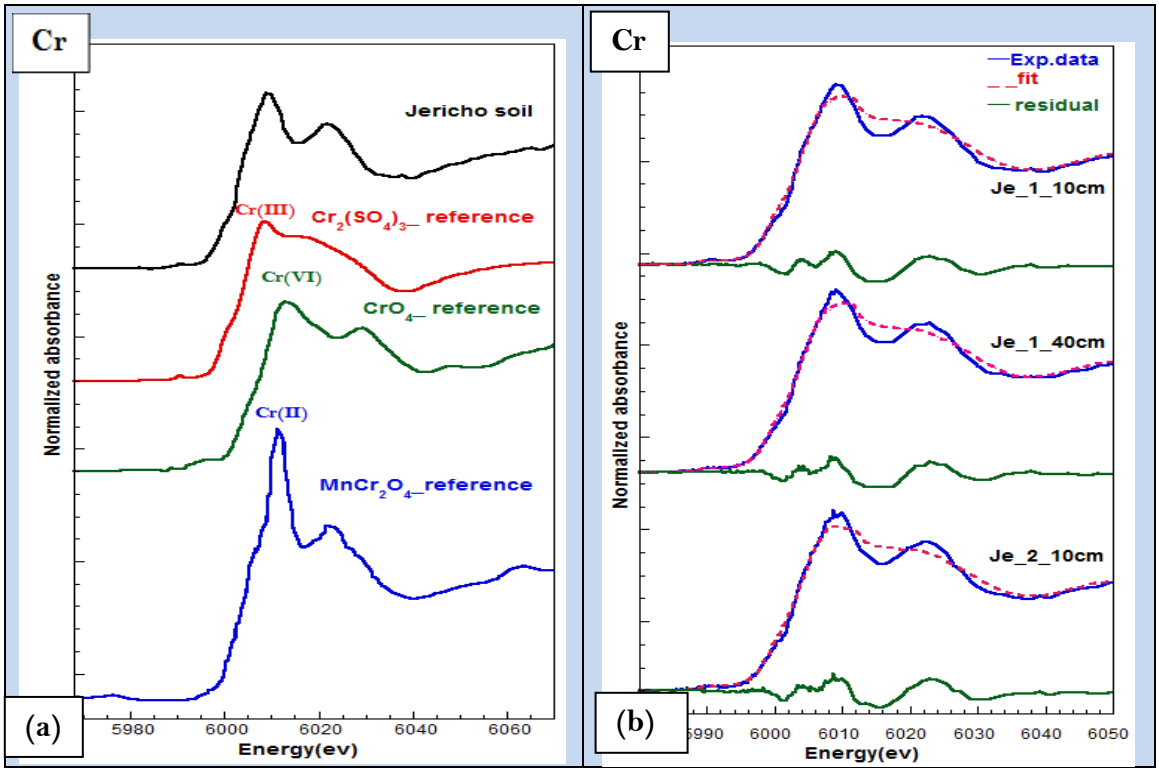

Figure 4.1: a) XANES spectra of different Cr model compounds compared to the XANES of a soil sample b) Linear combination fitting of the experimental XANES data collected on soil samples from Jericho.

The reference materials using for fitting are Cr2(SO4)3(chromium (III) sulfate), MnCr2O4(Manganese Chromate (II) and Cr(OH)3 (Chromium(III) oxy-hydroxide), Key features of the XANES spectrums are similar, so Cr in collected Jericho soil have same species and same oxidation state, the comparison the spectra of Cr in the soil to reference spectra in-

dicates that Cr is mainly comprising the (III) form. However, other Cr species can occur since the XANES fit is not to the best because of lake in model compounds data.

Linear Combination Fitting Results

Table.4.1 Shows LCF Results for Jericho soils, linear combination fitting (LCF) within an energy range of −20 eV below to +110 eV above the edge for all samples.

Table 4.1: linear combination fitting (LCF) results of Jericho samples.

Je_1_10cm R-factor = 0.002454		**Je_1_40cm** R-factor = 0.002362		**Je_2_10cm** R-factor = 0.002587	
compound	**percent**	**compound**	**percent**	**compound**	**percent**
$Cr_2(III)(SO_4)_3$	0.292	$Cr_2(III)(SO_4)_3$	0.307	$Cr_2(III)(SO_4)_3$	0.274
$Cr(III)(OH)_3$	0.610	$Cr(III)(OH)_3$	0.606	$Cr(III)(OH)_3$	0.627
$MnCr_2(III)O_4$	0.098	$MnCr_2(III)O_4$	0.087	$MnCr_2(III)O_4$	0.099

The analysis suggests that the majority of the species of chromate are Cr(III), chromate is toxic to plants, animals and humans and is a suspected carcinogen, whereas Cr(III) is not toxic to plants and is necessary in animal nutrition.

4.1.2 EXAFS Data Analysis

A comparison of the experimental Cr k-edge EXAFS spectra and their corresponding Fourier Transforms for Jericho soil of Figure 4.2 indicates some minor differences where the local structure occurs in a number of neighboring atoms and their interatomic distance around Cr. This is clearly visible in the FT in particular at the 2^{nd} and 3^{rd} shells in **Je-2-10cm**, **Je-3-10cm** and **Je-1-40cm** samples.

The first peak in the FT is the contribution of the nearest-neighbor oxygen atoms. It is well separated from the distant second nearest-neighbor peak of Cr. FT shows the splitting of the second shell shown by the double peaks in the **Je-1-40cm**, **Je-2-10cm** and **Je-3-10cm** spectra. The **Je-3-10cm** to **Je-2-10cm** and **Je-1-40cm** to **Je-1-10cm** spectra also show that the relative amplitude of the peaks decreases as R increases. The periodic oscillations also become more washed out as R increases indicating atoms become more disordered.

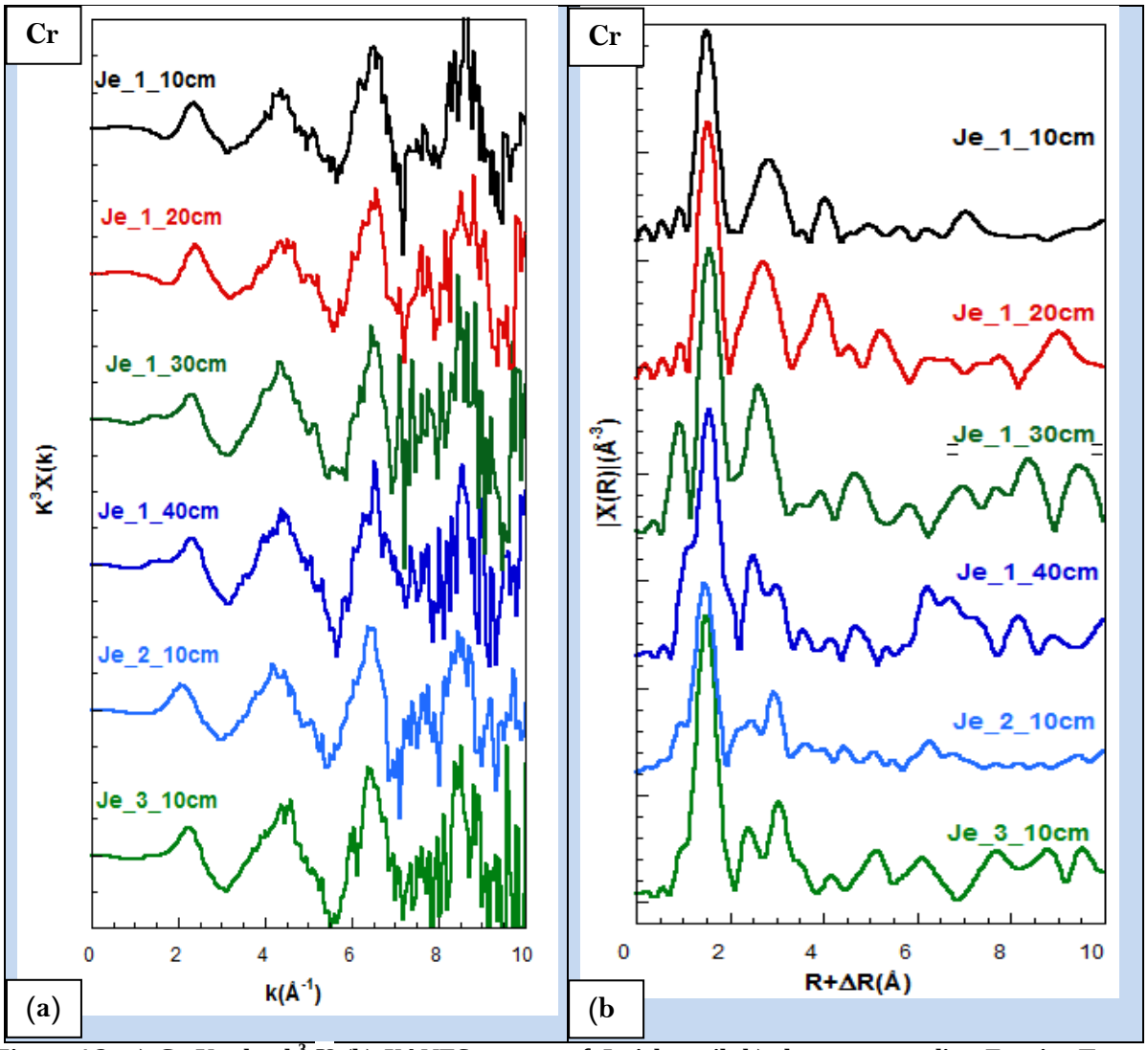

Figure 4.2: a) Cr-K edge k^3 X (k) XANES spectra of Jericho soil. b) the corresponding Fourier Transforms.

EXAFS Spectrum Fitting

To determine the types of species present in Jericho soils, we carried out a curve fitting of the EXAFS data collected at Cr k-edge containing reference compounds. FT of the experimental EXAFS data (at Cr K-edge) of the Jericho soil sample and the best fit to data are shown in Figure 4.3. The fitting was performed for the first three nearest neighboring shells using the photoelectron single scattering path of the crystalline [MnCr2(II)O4] model. Namely the Cr–O path at 1.994 Å, Cr-Cr path at 2.946 Å and Cr-Mn path at 3.455 Å. The FT was performed in the k range of 1.0-11.0 $Å^{-1}$ and main peaks were observed at 1.6 Å for all the samples. The amplitude of all theoretical EXAFS spectra was scaled by $\mathbf{S^2_0=0.9}$, which estimated from the prior analysis of the first shell Cr–O EXAFS signal.

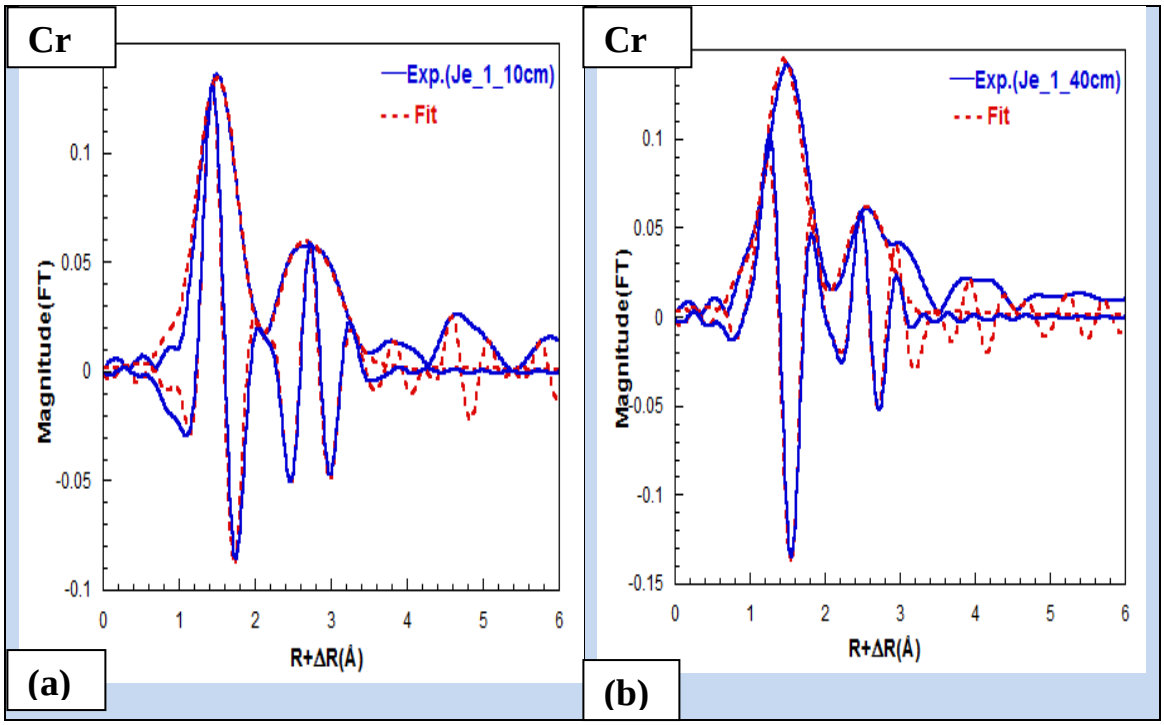

Figure 4.3: Comparing a) the magnitude and real part of the Fourier Transform of Cr K-edge experimental EXAFS spectra are shown in solid lines for Je-1-10cm with b) Je-1-40cm with theoretical EXAFS spectrum fitting that shown in dotted lines

The fitting results of the Cr K-edge EXAFS spectra are listed in Table 4.2. EXAFS simulations describe the structure around Cr very well. From Table (4.2) the analysis of the Jericho samples contain a significant oxide component that is reproducing well the EXAFS spectrum phase.

Table 4.2: Structural parameters obtained from the curve-fitting, *N*, *R*, σ^2, and ΔE: are coordination numbers, Interatomic distance, Debye-Waller factor, and Shifts of the threshold energy respectively.

Samples	Shell	N (atoms)	R (Å)	σ^2 (Å^2)	ΔE (eV)
Je_1_10cm	Cr-O	5.4±0.5	1.98±0.02	0.0035	4.80±2
	Cr-Cr	4.3±0.5	3.06±0.02	0.0078	4.80±2
	Cr-Mn	6.74±0.5	3.41±0.02	0.0160	4.80±2
Je_1_40cm	Cr-O	4.8±0.5	1.94±0.02	0.0024	3.72±2
	Cr-Cr	3.08±3	3.04±0.02	0.0102	3.72±2
	Cr-Mn	1.73±3	3.40±0.02	0.026	3.72±2

At 10 cm depth from Cr atoms are surrounded by light elements at short distance of about ~ 6 oxygen atoms sitting at the interatomic distance of ~2 Å from the central Cr atom. Other backscattering show atoms presence of ~ 4 Cr at a distance of ~ 3 Å. The interatomic distances are accurate, although we speculate that their accuracy decreases with the increase of the distances.

Further EXAFS results for the next nearest neighbors with semi-quantitative analysis show a presence of ~7 Manganese backscattering atoms around Cr at an interatomic distance of ~3.4Å, while at depth of 40 cm Cr appeared to be surrounded by 4.8 oxygen atoms at 1.94 Å. The next nearest neighbors are 3 Cr atoms at distance ~ 3 Å and 1.7 Manganese atoms at distance ~ 3.4Å. In general, the number of Manganese backscattering atoms around Cr decrease with depth.

The Manganese(II) Chromate [MnCr2(II)O4] model of crystalline structure shows spinel-like structure and cubic symmetry. There are 6 near-neighbor oxygen atoms that sit at 2Å from the central Cr atom. There are also 6 neighboring Cr atoms at an interatomic distance of 2.94Å from the central Cr atom, in addition to 6 neighboring Mn atoms at an interatomic distance of 3.45Å from the central Cr in a good agreement with results of Table 4.2.

4.2 Studying Mn of Qalqilia Samples

4.2.1 XANES Data Analysis

Figure 4.4 shows normalized Manganese (XANES) spectra that have K-edge peak energies between 6551.5 and 6557.2 eV. Key features of the XANES spectra are similar, and hence Mn in collected Qalqilia soil has the same species and oxidation state.

The reference compound spectra used to fit the experimental XANES data are Manganese(III) oxide (Mn2O3), Manganese(IV) dioxide (MnO2), Manganese(II), Carbonate (MnCO3), Manganese (II) Sulfate Monohydrate (MnSO4-H2O). The comparison of the Mn spectra of Mn for all Qalqilia samples with reference spectra indicates that Mn (3+) and Mn (4+) are the most dominating oxidation forms. Meanwhile, Manganese is also present in its divalent form as a carbonate.

Linear Combination Fitting Results (LCF)

LCF was performed within an energy range of −20 eV below to 110.00 eV above the edge Mn K-edge for Qalqilia soil. Results derived from the LCF analysis are shown in Table (4.3) indicate Mn in Qalqilia soils occurs mainly in trivalent (3+) and tetravalent (4+) forms. More specifically, Mn(III) oxide predominates in **Qal-2-10cm** (50%), Mn(IV) oxide predominates

in **Qal-1-10cm** (57%), also Mn(IV) oxide predominates in **Qal-1-40cm** (51%), In general, Mn in Qalqilia soils is in Mn(IV) and Mn(III) oxidation state.

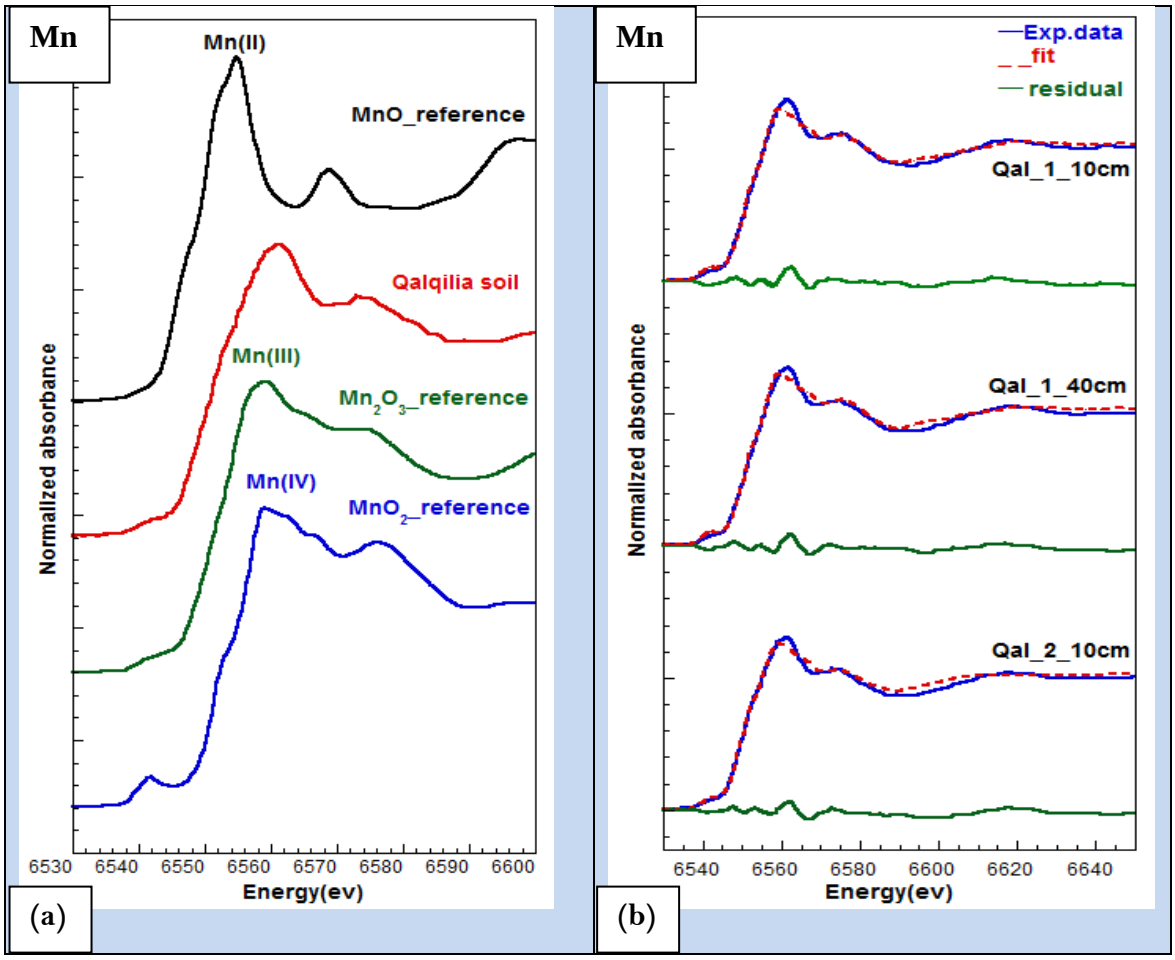

Figure 4.4: a) XANES spectra of different Mn model compounds compared to the XANES of a soil sample b) Linear combination fitting of the experimental XANES data collected on soil samples from Qalqilia.

Table 4.3: linear Combination Fitting (LCF) results of Qalqilia soils.

Qal_1_10cm R-factor= 0.000898		**Qal_1_40cm** R-factor = 0.001036		**Qal_2_10cm** R-factor = 0.000938	
Compound	**percent**	**Compound**	**percent**	**Compound**	**percent**
$Mn^{3+}2O3$	0.343	$Mn^{3+}2O3$	0.388	$Mn^{3+}2O3$	0.499
$Mn^{4+}O2$	0.565	$Mn^{4+}O2$	0.514	$Mn^{4+}O2$	0.342
$Mn^{2+}CO3$	0.081	$Mn^{2+}CO3$	0.098	$Mn^{2+}CO3$	0.159

4.2.2 EXAFS Data Analysis

Comparison of the experimental Mn k-edge EXAFS spectra of Qalqilia soil of Figure 4.5 indicates good agreement in the shape of EXAFS spectra. The soil has similarity in the local environment structure around Mn.

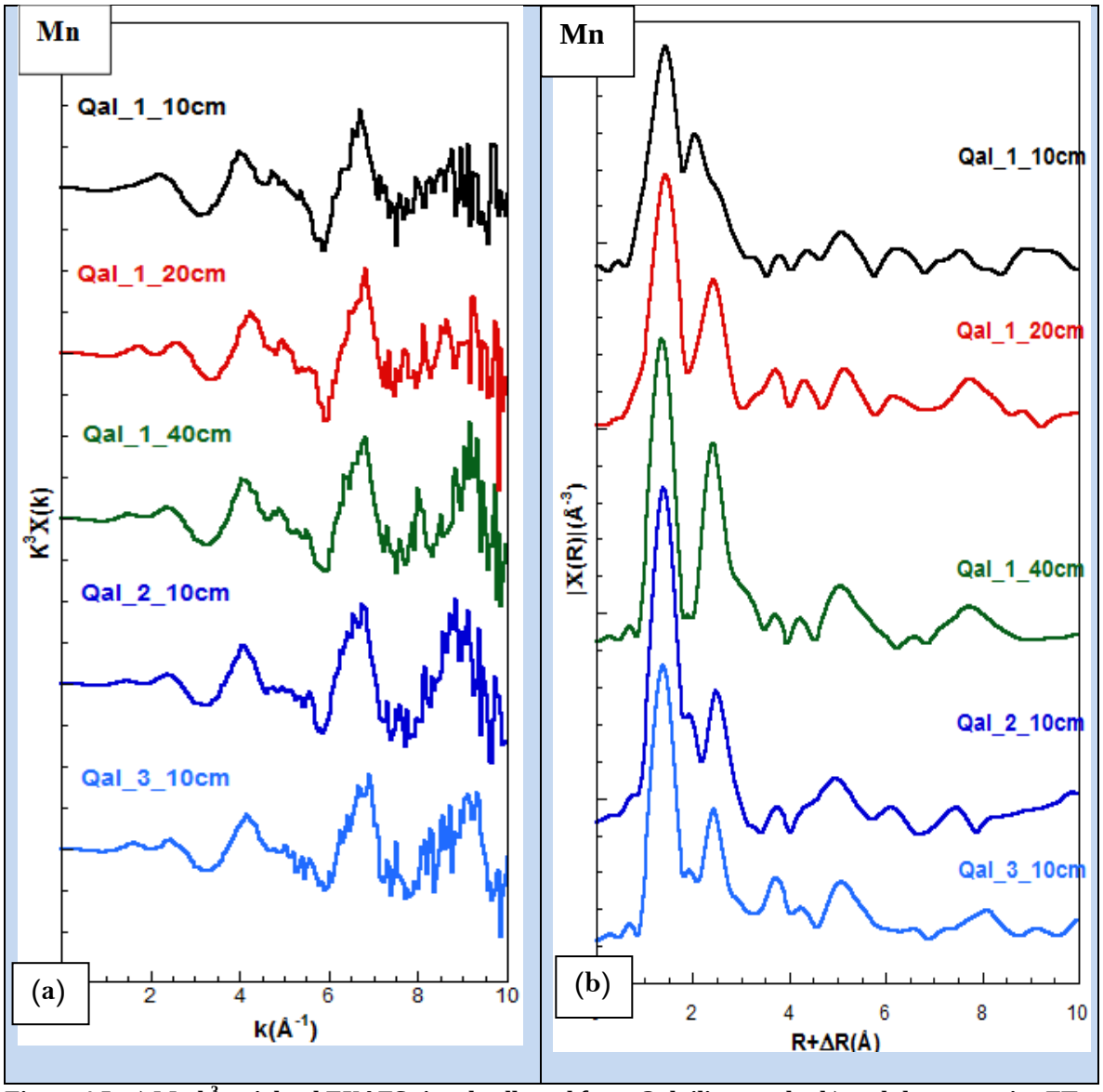

Figure 4.5: a) Mn k^3 weighted EXAFS signal collected from Qalqilia samples b) and the respective FTs

EXAFS data Fitting

In order to understand the local structural order around Mn in Qalqilia soil, a curve fitting analysis of the EXAFS data collected at Mn K-edge. FT of experimental EXAFS data (at Mn K-edge) of the Qalqilia soil sample and the best fit to data is shown in Figure 4.6. The fitting was performed on the first three nearest neighboring shells using the single scattering photoelectron path of the crystalline model of Mn [C2O4]. The model structure is ordered as a coordination shell Mn–O path at 1 .753Å, Mn-Mn of path at 3.292 Å and Mn-C path at 2.922 Å.

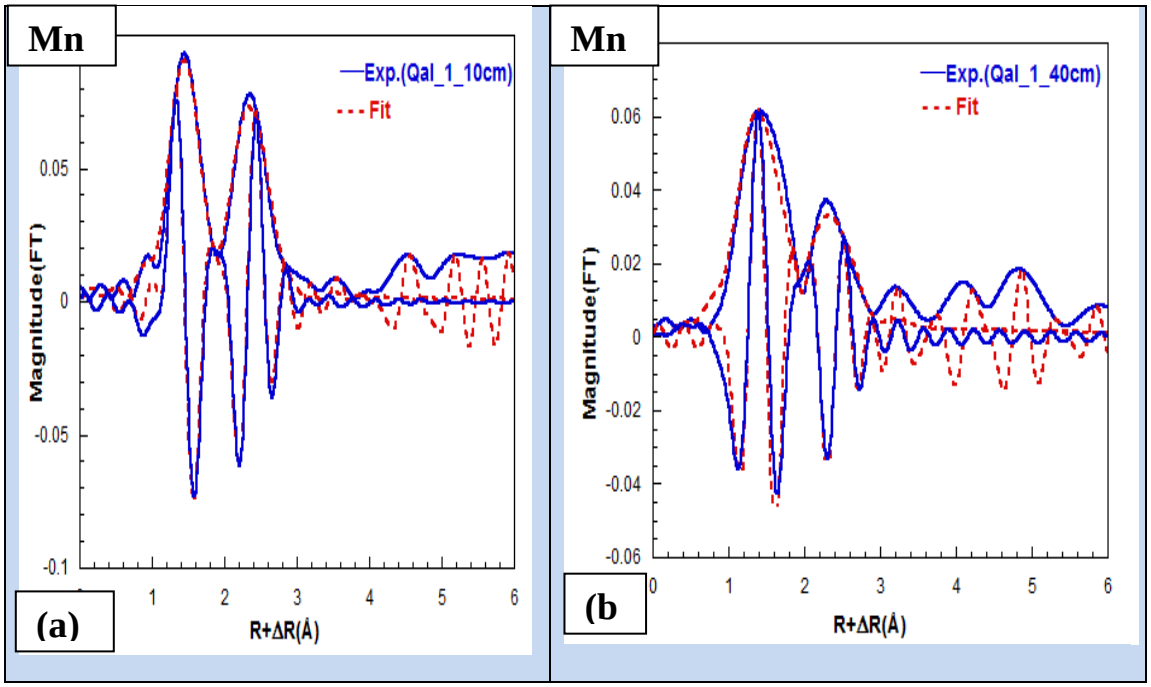

Figure 4.6: Fitting the Fourier Transformed EXAFS signal, collected from Qalqilia samples as a function of depth.

The EXAFS signal FT is in a wavenumber range k of 1.0-11.0 $Å^{-1}$. Distinguished magnitude peaks of the FT are observed at 1.6 and 2.4 Å for all the samples. To reduce the number of floating parameters, $\mathbf{S^2_0}$ was fixed to 0.9 value. The fitting results of the Mn K-edge EXAFS spectrum Qalqilia are listed in Table 4.4.

Table 4.4: EXAFS derived structural parameters (*N*, R, σ^2, ΔE) around Mn in Qalqilia soil samples.

Samples	Shell	N (atoms)	R (Å)	σ^2 ($Å^2$)	ΔE (eV)
Qal_1_10cm	Mn-O	3.2±0.5	1.90±0.02	0.00052	5.51±2
	Mn-Mn	3.4±0.5	2.81±0.02	0.0033	-1.68±2
	Mn-C	12.9±0.5	2.91±0.02	0.0084	-19.24±2
Qal_1_40cm	Mn – O	3.9±0.5	1.82 ±0.02	0.00093	4.98±2
	Mn-Mn	3.2±3	2.87±0.02	0.00621	4.68±2

At 10 cm depth Mn are surrounded by light elements at close distances and appeared to be ~4 O atoms at a distance of ~2Å from the central Mn, and ~4 Mn-Mn bound at a distance of~ 2.8Å. The interatomic distances are accurate, although we speculate that their accuracy decreases with the increase of the distances. EXAFS results for the next nearest neighbors for semi-quantitative analysis, show a presence of 13 Mn-C backscattering atoms around Mn at an interatomic distance of ~3Å in agreement with LCF results. At the depth of 40 cm Mn appeared to be surrounded by 4 oxygen atoms at 1.8Å, ~3 Mn-Mn bound at a distance of~ 2.9Å,

Mn-C disappears and Mn-O interatomic distances are smaller. MnO2 model crystalline structure shows 6 near-neighbor oxygen atoms that all sit at 1.75Å from the central Mn atom. There are also Mn-O bond at an interatomic distance of 2.63Å from the central Mn atom, also Mn-Mn bond at an interatomic distance of 2.78Å from the central Mn atom, indicating shorter bond compared to the results of Table 4.4.

4.3 Studying Mn of Hebron Samples

4.3.1 XANES Data Analysis

Figure 4.7a Shows Mn K-edge normalized XANES spectra of Hebron samples comparisons with some reference Mn compounds. The unknown Mn k-edge XANES spectra represent linear combinations of the reference compound spectra as shown in Figure 4.7b. The dotted lines represent the LCF curves, which closely resemble the original spectrum.

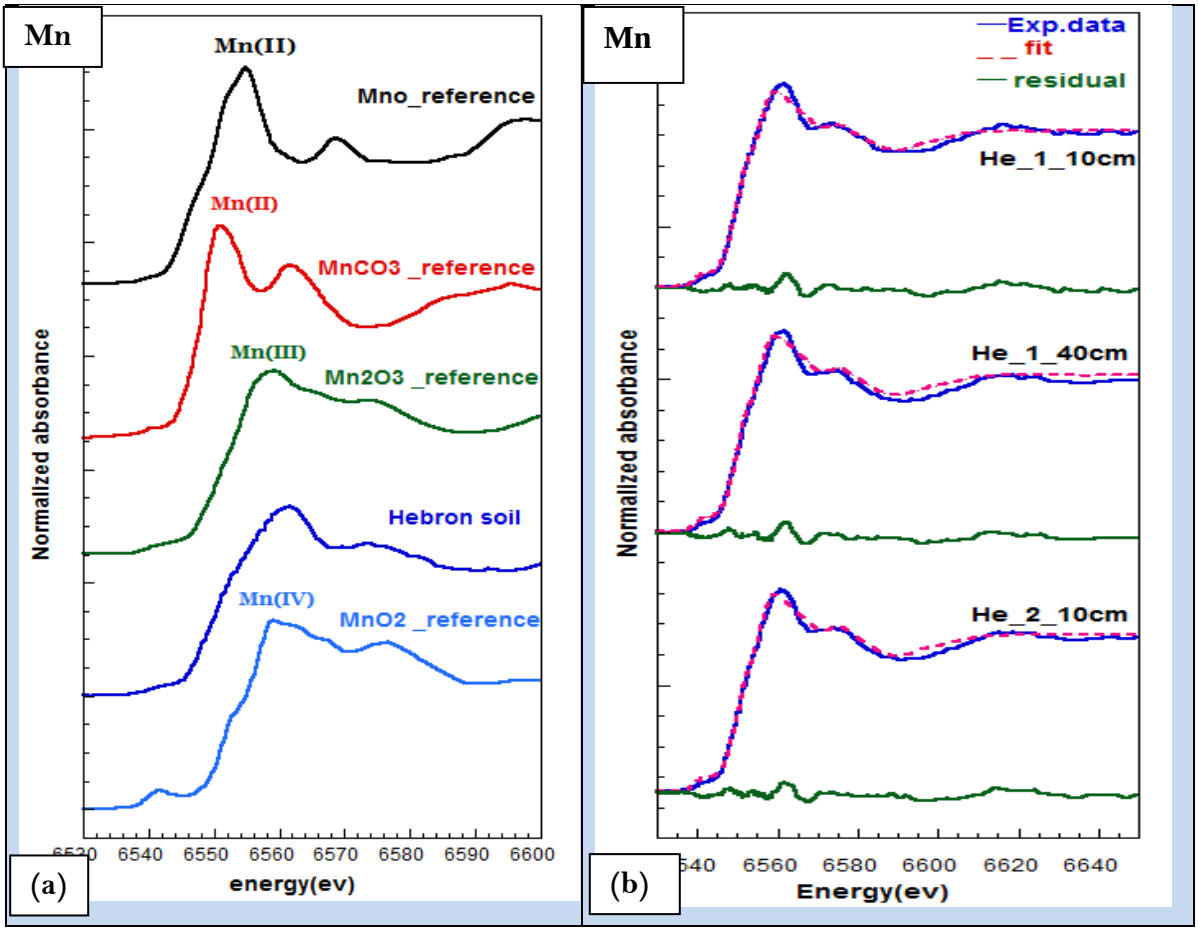

Figure 4.7: a) Mn K-edge normalized XANES spectra of Hebron samples comparisons with reference Mn compounds. b) the unknown Mn k-edge XANES spectra are expressed as linear combinations of the reference compound spectra. The dotted lines represent the LCF curves, which closely resemble the original spectrum.

The reference compound spectra used in the fitting are Manganese (III) oxide (Mn2O3), Manganese (IV) dioxide (MnO2), Manganese (II) Carbonate (MnCO3), and Manganese (II) Sulfate Monohydrate (MnSO4-H2O).

LCF was made for the energy range of −20 eV below to 110.00 eV above the Mn. The fit revealed that Mn takes mainly 3+ and 4+ forms. The results of the LCF analysis of Hebron samples are shown in Table 4.5 indicate the presence of Mn as a combination of three oxidation states. Mn (III) dominates species with concentration around 50% for all samples. Mn(IV) presence ranges from 30-40 %. The Mn (II) concentration of about 15%.

Table4.5: Linear combination fitting results of Hebron soil.

He_1_10cm R-factor = 0.000785		**He_1_40cm** R-factor = 0.001726		**He_2_10cm** R-factor = 0.001037	
compound	**percent**	**compound**	**percent**	**compound**	**percent**
$Mn^{3+}2O3$	0.499	$Mn^{3+}2O3$	0.482	$Mn^{3+}2O3$	0.494
$Mn^{4+}O2$	0.334	$Mn^{4+}O2$	0.371	$Mn^{4+}O2$	0.384
$Mn^{2+}CO3$	0.167	$Mn^{2+}CO3$	0.147	$Mn^{2+}CO3$	0.121

4.3.2 EXAFS Data Analysis

Experimental EXAFS spectra collected at Mn k-edge in Hebron soil samples and their corresponding Fourier Transform are shown in Figure 4.8. Comapraison of the data collected at different sites and depths shows some similarities in the first neigboring shell but a clear difference in the other shells of the backscattering neighbors.

EXAFS Data Fitting

The data fitting used theoretical reference models with well-defined crystalline structures and calculation was made using FEFF. The best fits to experimental EXAFS spectra of Hebron soils at Mn K-edge are shown in Figure 4.9. The fitting was performed for the first three nearest neighboring shells using the photoelectron scattering single path of the crystalline model of Mn[C2O4], More specifically, a Mn–O path at 1 .75Å, Mn-Mn path at 3.292Å, and Mn-C path at 2.92Å.

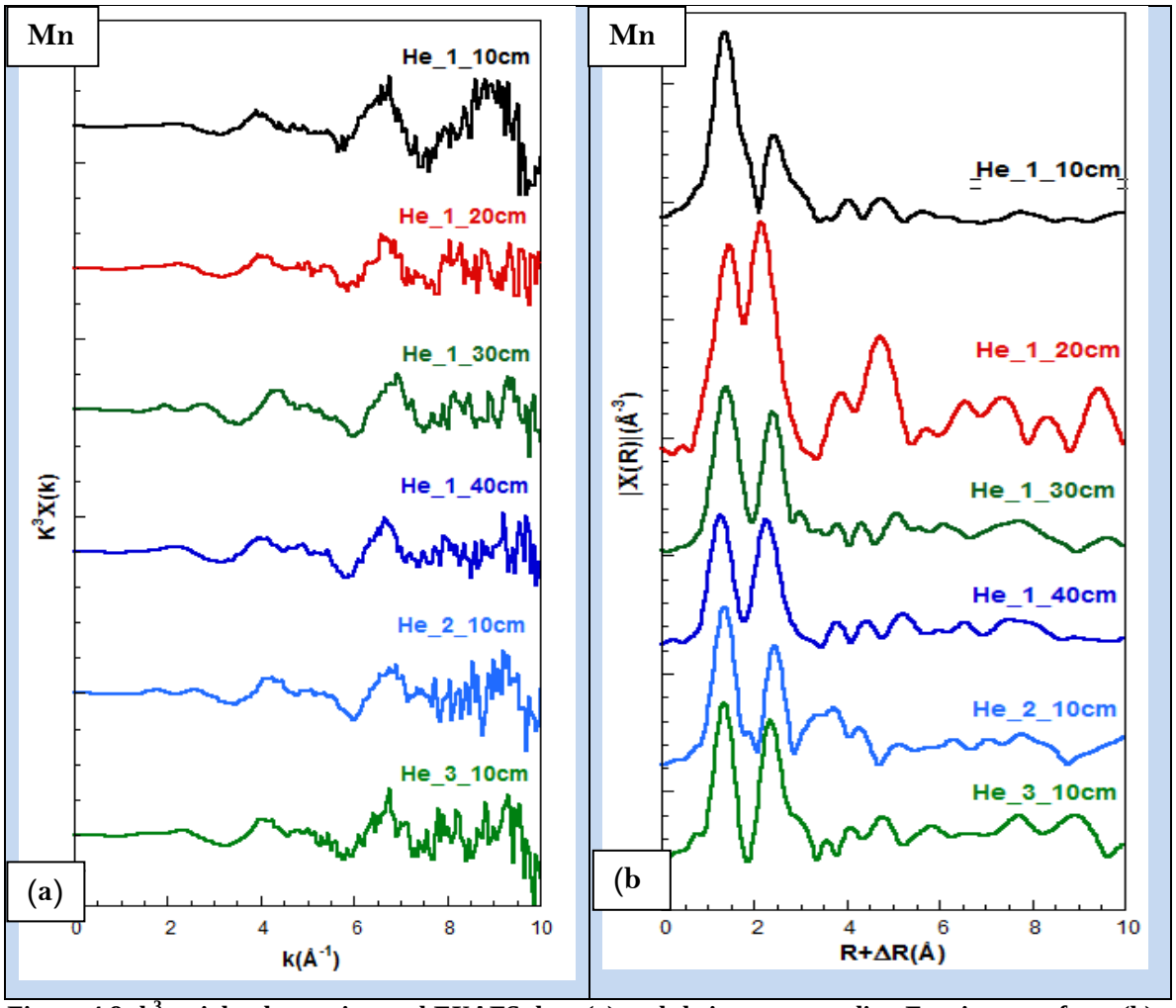

Figure 4.8: k^3 weighted experimental EXAFS data (a) and their corresponding Fourier transform (b) collected at the Mn K-edge in soil samples from different sites in Hebron.

The Fourier transformation was performed in the K range of 1.0-11.0 Å-1. Distinguished magnitude peaks of the FT are observed at 1.6 Å and 2.4 Å for all the samples. The amplitude of all theoretical EXAFS spectra was multiplied by the scale factor S^2_0 = 0.9 estimated from prior analysis of the first shell Mn–O EXAFS signal**.** Figure 4.6 shows the results.

Table 4.6: Structural parameters (*N*, R, σ^2, ΔE) in Hebron soil samples obtained by the curve-fitting.

Samples	Shell	CN	R (Å)	σ^2 (Å^2)	ΔE (eV)
He_1_10cm	Mn-O Mn-O Mn-Mn Mn-C	3.8±0.5 1.7 ±2 7.3±0.5 13.2±0.5	1.87±0.02 2.06±0.02 2.87±0.02 3.04±0.02	0.00232 0.00232 0.01231 0.0096	6.37±2 -6.33±2 6.37±2 -6.33±2
He_1_40cm	Mn – O Mn-Mn	4.1±0.5 3.6±3	1.85 ±0.02 2.82±0.02	0.00663 0.00661	5.68±2 5.68±2

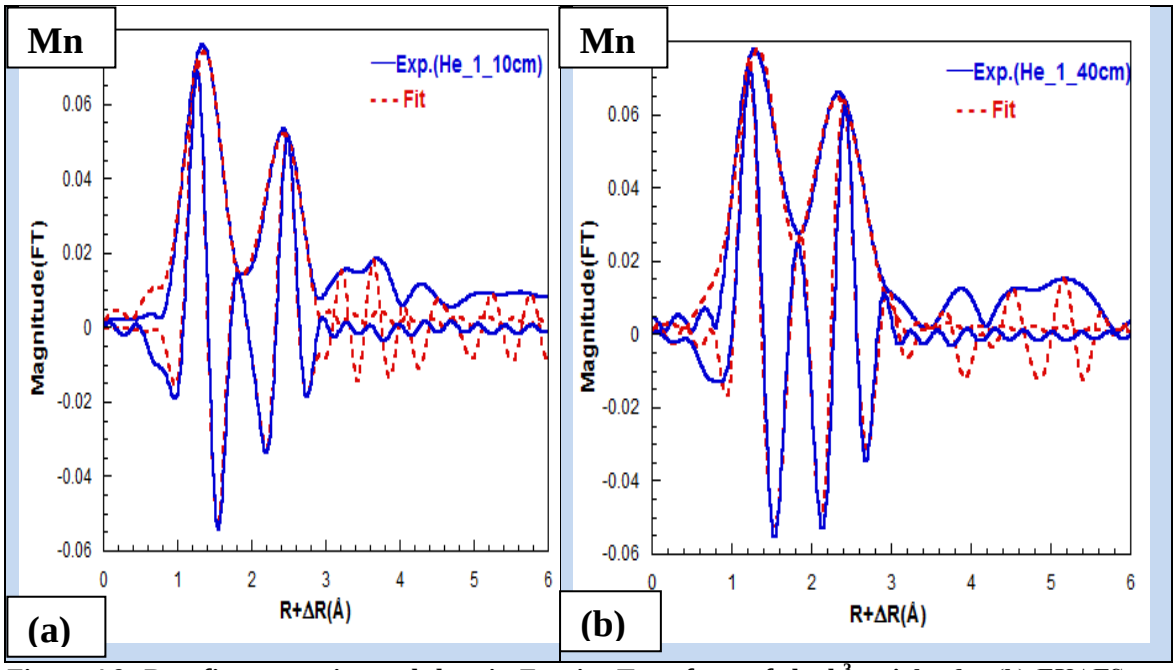

Figure 4.9: Best fit to experimental data in Fourier Transform of the k^3 weighted χ (k) EXAFS spectra recorded at the Mn K-edge on soil samples from Hebron.

The sample at 10cm depth Mn atoms are surrounded by ~6 O atoms in a double shell at 2 different distances ~1.89 Å and ~2 Å. Only one shell Mn-O in the 40cm depth has shorter distance 1.85 Å and only 4 atoms. The ~13 atoms of C backscatters on the 10cm sample indicates bioavailability near the surface which is not the case for the 40cm depth.

4.4 Studying Zn of Jericho Samples

4.4.1 XANES Data Analysis

XANES spectra data were collected at Zn K-edge (9659 eV) in soil samples from Jericho. Figure 4.10 shows the normalized XANES spectra from soil samples compared to similar well defined reference models for Zn in addition to the best fit of the spectra using LCF. Table 4.7 results show Zn presence in a form similar to a 50 /50 mix of ZnOH and ZnO4C2.

Table 4.7: LCF results of Jericho soils

Je_1_10cm R-factor =0.003157		**Je_1_40cm.** R-factor= 0.00227		**Je_2_10cm** R-factor = 0.00197	
compound	**percent**	**compound**	**percent**	**compound**	**percent**
Zn (OH)	0.537	Zn(OH)	0.524	Zn(OH)	0.423
ZnO_4C_2	0.463	ZnO_4C_2	0.476	ZnO_4C_2	0.57

EXAFS Data Analysis: Figure 4.11 shows the K EXAFS signals recorded at Zn K-edge in Jericho soils and their respective Fourier Transforms. Small differences of the Zn k^3 weighted EXAFS signals from different sites are seen. And more pronounced at higher k (>8 $Å^{-1}$). The comparison between the Fourier transform of the EXAFS signal shows similarities at short and medium range order. Significant differences may occur in the number of neighboring atoms around Zinc.

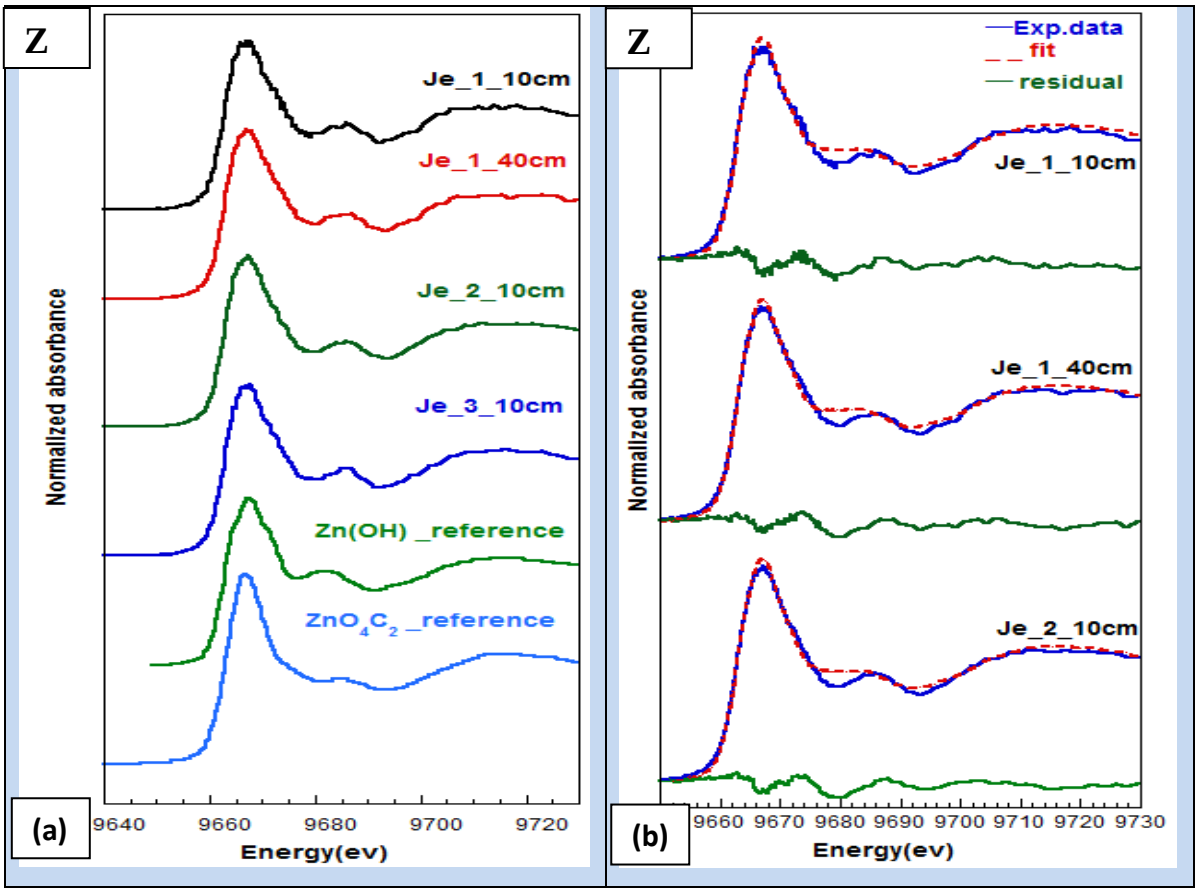

Figure 4.10: Normalized XANES spectra collected at Zn K-edge in soil samples from Jericho. a) Comparisons between soil samples and some Zn reference compounds. b) Best fit to data using LCF.

EXAFS Spectrum Fitting: Figure 4.12 shows the FTs of 2 samples from Jericho site at 2 different depths with the resulting best fit to data. The EXAFS signal FT was made for k range from 1.0-11.0 $Å^{-1}$. Main features were observed at 1.5Å and 2.5 Å of the FT. The amplitude of all theoretical EXAFS spectra was multiplied by the scale factor $\mathbf{S^2_0=0.9}$, estimated from the prior analysis of the first shell Zn–O EXAFS signal. EXAFS backscattering paths around Zn in theoretical crystalline structures (ZnC2O4, and Zn3[PO4]2) were calculated and used to fit the experimental EXAFS data of Figure 4.12.

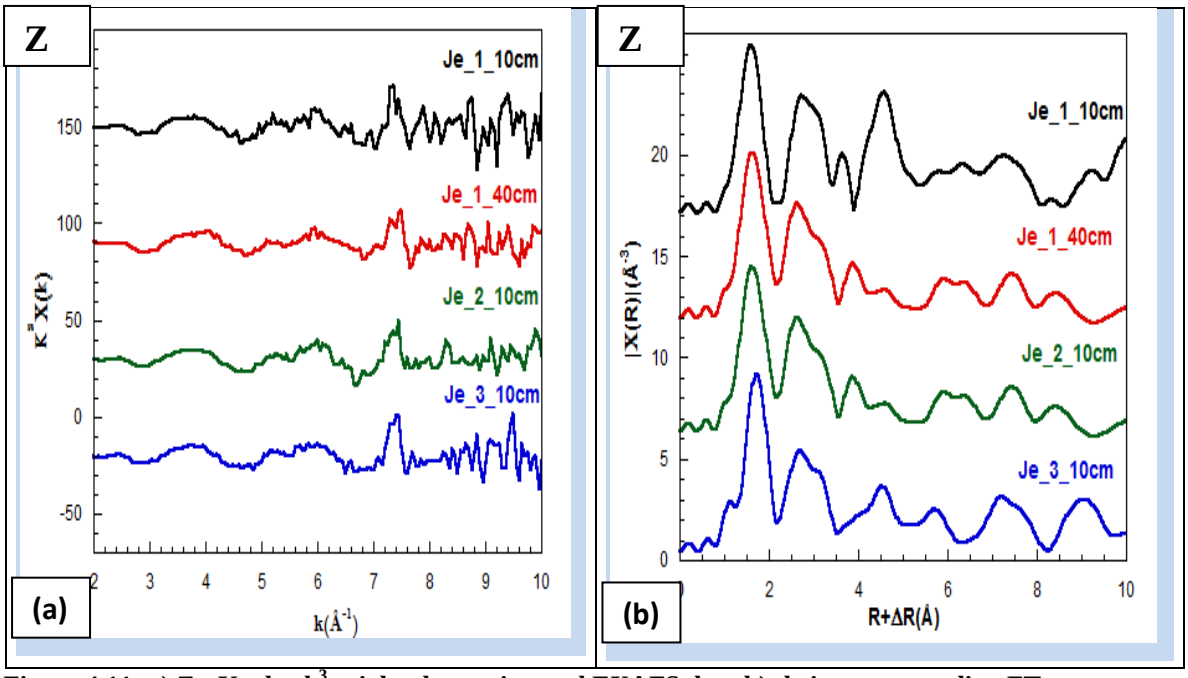

Figure 4.11: a) Zn-K edge k^3weighted experimental EXAFS data b) their corresponding FTs.

The ZnC2O3 model was used to fit the shells with O, C and Zn backscatters, namely Zn–O path at 2.105 Å, Zn–C path at 2.964 Å and Zn-Zn path at 3.324 Å. Zn3[PO4]2 Model compound was used for modeling P shell (Zn-P path at 2.963 Å). Results are shown in Table 4.8.

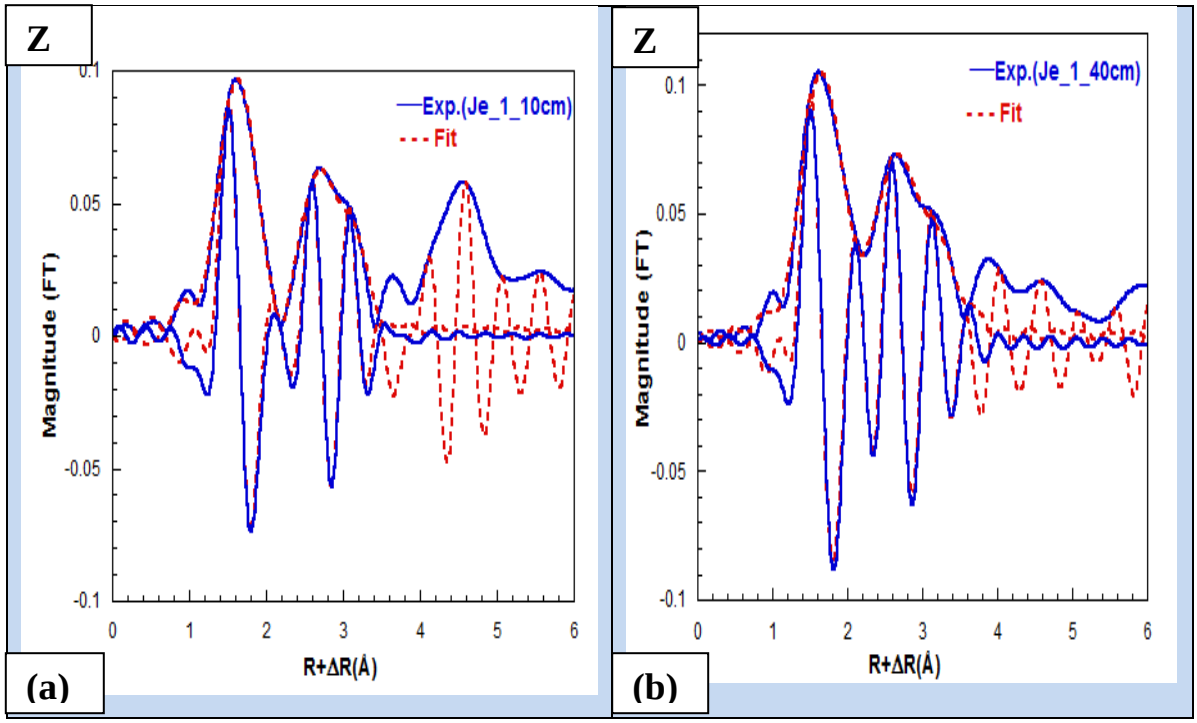

Figure 4.12: a) Modeling the local structure around Zinc atoms in soil samples from Jericho collected from the surface. b) at 40 cm depth.

Table 4.8: Structural parameters (*N* ,*R*, σ^2, ΔE) of Jericho obtained by the fitting the EXAFS data.

Samples	Shell	N(atoms)	R (Å)	σ^2 ($Å^2$)	ΔE (eV)
Je_1_10cm	Zn – O	3.2±0.5	2.06±0.02	0.00107	3.66±2
	Zn– C	19.2±3	2.96±0.02	0.00664	-13.23±2
	Zn – P	5.3±0.5	3.06±0.02	0.00207	-0.89±2
	Zn-Zn	3.3±0.5	3.40±0.02	0.00661	3.66±2
Je_1_40cm	Zn – O	3.6±0.5	2.06±0.02	0.00178	3.68±2
	Zn– C	18.1±3	2.94±0.02	0.00207	-14.58±2
	Zn – P	5.9±0.5	3.16±0.02	0.002075	-0.71±2
	Zn-Zn	2.5±0.5	3.46±0.02	0.00681	3.68±2

4.5 Discussion

The elemental content chemical analysis showed that Some heavy metals are not in the contamination limit, and other of heavy metals are in the tolerant contamination range Knowing the local structure around some of the heavy metals in soil will reveal good information about the soil system in the region.

4.5.1 Jericho Chromium XAFS

XANES data collected at the Cr K-edges in Jericho were subject to LCF using different experimental model compounds shows that Cr is present in a form similar to $Cr(III)(OH)_3$, $MnCr2(II)O_4$ and $Cr_2(III)(SO_4)_3$-like with content distributed for the phases as ~63%, 10% and 27% respectively.

Cr in Jericho Soils occurs mainly in divalent Cr(II) and/or trivalent Cr(III) forms which is are not-mobile or have reduced mobility. Moreover, Cr in its hexavalent (VI) form is not present. The EXAFS results showed no variation in the local structure around Cr as a function of depths because Cr-O, Cr-Cr and Cr-Mn are present with the same distance at all depths. Cr was present in the $Cr(III)(OH)_3$ inorganic form. It is also present in the Manganese and Sulfurous structures. Organic ligands to Cr were not detected from all depths. This is an indication of non-bioavailability of Cr in Jericho samples. Jericho Soils have moderate Cr contamination and lower oxidation states Cr (II), Cr (III). This minimizes mobility and limits harmfulness.

4.5.2 Jericho Zinc XAFS

Zn is 2+ and can be harmful if the concentration exceeds the standard limits. Results showed a small difference between Jericho samples as a function of depth. In all analyzed samples Zn

is present in hydroxide Zn $(OH)_2$ or carbonate ZnO_4C_2-like forms with content distributed for the two phases equal to ~54% and 46% respectively. Zn species were not influenced by the agricultural processes despite the use of fertilizers. This can be an indication that Zn is present in an organic form because it binds to carbon as ($ZnO_4C_{2)}$. In general Zn occurs in a stable carbonate structure independent of the soil specifications. If Zn is linked to C, N, OH it is considered bioavailable.

EXAFS data for Zn in Jericho shows no variations as a function of the depth because Zn-O, Zn-C, Zn-P and Zn-Zn bonds were fitting data. Zn in general occurs in organic form with atoms surrounded by light elements such as O, C and P in agreement with LCF results. The number of carbon backscattering atoms found was high and thus not accurate due to the noise level of EXAFS spectra at high wavenumber (k). Carbonate or hydroxide forms mean Zn is bioavailable and can be absorbed by plants. The mechanism and metabolism of plants manage their uptake of metals which minimizes their harmfulness.

4.5.3 Qalqilia and Hebron Manganese XAFS

XANES spectra of Mn collected at k- edge from Qalqilia show that Mn generally occurs in Mn(IV) and Mn(III) oxidation states as oxide or carbonate forms ($Mn(III)_2O_3$, $Mn(IV)O_2$ and $Mn(II)CO_3$ -like). This can indicate that Mn may be present in an organic form because it binds to carbon $Mn(II)CO_3$(17%).

They also show that Mn is present in inorganic oxides [$Mn(III)_2O_3$, $Mn(IV)O_2$] with larger content. That shows some difference with results derived from XANES spectra of Mn from Hebron Soils which have Mn present in an organic and inorganic phases as oxides or carbonates or combination of three oxidation states. Mn (III) is the dominating specie with concentration close to 50% in all probed samples. Results also presented higher values of Mn (IV) raging between 30-40%. The Mn (II) have a concentration of 15%.

In contrast to XANES, results derived from EXAFS analysis from Qalqilia Soils show a significant difference in the local structure around Mn as a function of the depth. At the surface (10cm depth) Mn in Qalqilia was present in a bioavailable organic phase binding with C and can be absorbed by plants. Deeper in soil (40cm depth) Mn is present in an inorganic oxide form, similar to Hebron Soils.

5 Conclusions and Future Work

5.1 Summary

XAFS technique is very powerful quantitative methods to determine not only the oxidation state of the pollutant but also the atomic structure in the soil systems around selective elements (Cr, Mn and Zn in our case). Therefore, XAFS techniques combined with other conventional techniques (ICP-MS), can identify many environmental problems. Synchrotrons are very important to improve scientific research quality and scope.

5.2 Conclusions

1. XAFS techniques are very reliable in analyzing many topics and they help solve many environmental aspects and problems. Establishing a Synchrotron facility is very important step for the well being of the region.
2. We have determined the concentrations and structures around the rare elements when we combined the conventional and Accelerator based analysis. We studied the chemical elements that can be found in a soil and project the atomic structure even in the amorphous phases by combining XAFS and other conventional techniques.
3. The three Manganese species were present as Mn_{III} close to 50%, Mn_{IV} around 30-40% and Mn_{II} was 15%. Mn in Qalqilia surface Soils is present in the organic phase which is bioavailable and can be absorbed by plants. In the deep soil however Mn is present in an inorganic oxide form. The last was also seen in the Hebron Soil.
4. Jericho Soil has moderate contamination of Chromium concentrations, occurring in the trivalent Cr_{III} form which is not mobile. The toxic hexavalent Cr_{VI} form is not present in the soil samples.
5. No organic ligands to the Cr were measured in the soil at all depths indicating non-bioavailability of Cr in Jericho Soils.

6. Zn can be harmful beyond some levels. In all samples Zn is present as hydroxide $Zn(OH)_2$ and carbonate ZnO_4C_2. Zn species were not influenced by the agricultural processes despite the use of fertilizers indicating Zn is present in organic form. EXAFS results for Zn in Jericho confirm the same conclusion. Zn presence in a carbonate or hydroxide forms means it is bioavailable and the plants metabolism minimizes their harmfulness.

5.3 Future Work

We recommend extensive and more systematic studies of the Palestinian lands concerning other metals and possible toxicants and a continuation of the study through the productive collaboration with SESAME. Specific studies can be carried out applying similar methods including the use of X-ray absorption spectroscopy to study Cr mixed ligands, in addition to Iron, Lead and Copper complexes.

References

[Abhijeet , 2013] Abhijeet Gaur., B D Shrivastava., and H Lnigam. *"X-Ray Absorption Fine Structure (XAFS) Spectroscopy – A Review"*, Proc Indian Natn Sci Acad, Spl. Issue, Part B, pp. 921-966, 2013.

[Abu-Rukah , 2000] Abu-Rukah, Y., and Ghrefat, H.A. (2000). *"A study of the heavy metals distribution and fractionation in sediments of the Yarmouk River-Jordan"***,** Africa Geoscience Review, Vol.7, No.1, pp. 91-100, 2000.

[Aelion C.M,2003] Aelion C.M, *"Soil Contamination Monitoring Environmental Monitoring – Vol. II"* University of South Carolina ,Columbia,SC,USA,2003.

[Aksenov ,2001]V. L. Aksenov., A. Yu. Kuzmin., J. Purans., and S. I. Tyutyunnikov. *"EX-AFS Spectroscopy at Synchrotron-Radiation Beams"***,** Physics of Particles and Nuclei, Vol. 32, No. 6, 2001, pp. 1–33.2001.

[Alian A, 1996] Alian A Manceau., Marie-Claire Boisset., Geraldine Sarret., Jean- Loui ShazemannH., Michel Mench., Philippe Cambier., and Rene Prost, "*Direct Determination of Lead Speciation in Contaminated Soils by EXAFS Spectroscopy",* Environ. Sci. Technol, 30, 1540-1552 , 1996.

[Alsmadi, 2001] Alsmadi, Bashar M., Fox, Peter, **"***Semi-quantitative analysis of changes in soil coatings by scanning electron microscope and energy dispersive X-ray mapping. Colloids and Surfaces"*, A: Physicochemical and Engineering Aspects, Vol. 194 Issue (1-3), 249-261,2001 .

[Andrej, 2002] Andrej Miheli˘c., Alojz Kodre**.** *"XANES spectroscopy",* http://www.ung.si/~arcon/xas/xanes/xanes-theory.pdf , 2002.

[Brian Murphy, 2008] Brian Murphy, *"Key soil functional properties affected by soil organic matter evidence from published literature",* NSW Office of Environment and Heritage, Cowra, NSW,Australia.2008.

[Chiroma, 2014]Chiroma T. M , Ebewele R. O . And Hymore F.K. *"Comparative Assessment Of Heavy Metal Levels In Soil, Vegetables And Urban Grey Waste Water Used For Irrigation In Yola And Kano"***,** February 2014.

[Fendorf, 1995] Fendorf, S.E**,** *"Surface reactions of chromium in soils and waters",* Geoderma 67, 55-71,1995.

[Frenkel, 2001] A. I. Frenkel and G. V. Korshin*. "Studies of effects of pH on complexation of copper with humic substances by EXAFS and XANES",* Royal Society of Chemistry, Cambridge, p. 227, 2001.

[Gilberto, 2004] Gilberto Vlaica and Luca Olivib*,"EXAFS Spectroscopy: A Brief Introduction",* CROATICA CHEMICA ACTA -2944, ISSN-0011-1643, 2004.

[Guillaume, 1999] Guillaume Morin., John B.O Stergren., Farid Juillot., Philippe Ildoefonse., Georges Calas., Andgordon E. Brown , *"XAFS determination of the chemical form of lead in smelter-contaminated soils and mine tailings: Importance of adsorption processes",* American Mineralogist**,** Volume 84, pages 420–434,1999.

[Jeffrey Lewis, 2010] Jeffrey Lewis., Jan Sjöström., Ulf Skyllberg and Lars Häggluna*."EXAFS analysis of Pb speciation in bullet-contaminated range soils"***.**2010.

[Leonard Perry,2003] Leonard Perry, Extension Professor, *" pH for the Garden",* University of Vermont Extension Department of Plant and Soil Science,2003

[Matthew Newville, 2004] Matthew Newville, *"Fundamentals of XAFS"* Consortium for Advanced Radiation Sources University of Chicag Chicago, IL,2004.

[M. Harfouche, 2009] M. Harfouche, J. Labanowski, F. Farges, E. van Hullebusch, C. Borca, D. Grolimund, F. van Oort, *"Assessment of Zn bioavailability: XAFS study on speciation of zinc-particulate organic matter associations in polluted soils",* J. Phys. Conf. Ser**.** 190, 012189, 2009.

[Rehr ,2000] J. J. Rehr and R. C. Albers, *"Theoretical approaches to x-ray absorption fine structure",* Department of Physics, University of Washington, Seattle, Washington,2000.

[Ressler , 1998] T. Ressler, *"WinXAS: a Program for X-ray Absorption Spectroscopy Data Analysis under MS-Windows ",* J. Synch. Rad,1998

[Senesi, 1992] Senesi, N, *"Metal-humic substance complexes in the environment. Molecular and mechanistic aspects by multiple spectroscopic approach",* In: D.C. Adriano (ed),Biogeochemistry of Trace Elements. Lewis Boca Raton, FL, 1992.

[Soil Quality Institute, 1999] Soil Quality Institute*, "Soil Quality Test Kit Guide"*, United States Department of Agriculture Agricultural Research Service Natural Resources Conservation Service.1999.

[Tatiana A, 2006] Tatiana A. Kirpichtchikova, Alain Manceau., Lorenzo Spadini., Frederic Panfili., Matthew A. Marcus and Thierry Jacquet. *"Speciation and solubility of heavy metals in contaminated soil using X-ray microfluorescence, EXAFS spectroscopy",* chemical extraction, and thermodynamic modeling, Geochimica et Cosmochimica Acta, 70, 2163,2006.

[Violante et al, 2010] A. Violante, V. Cozzolino**,** *"Mobility and biovailability of HM and metalloids in the soil"***.** Dipartimento di Scienze del Suolo, della Pianta e dell'Ambiente, Università di Napoli Federico II, Portici (Napoli), Italy, 2010.

Internet References

[cfr.washington.edu]http://www.cfr.washington.edu/classes.esrm.410/moisture.htm.

[SESAME, 2016] http://www.sesame.org.jo.2016.

[Wikipedia] *http://en.Wikipedia.org.*

http://chemwiki.ucdavis.edu/Core/Physical_Chemistry/Spectroscopy/Xray_Spectroscopy/XANES%3A_Theory.

http://www.chemicalghosts.org/wp-content/uploads/2012/11/synchrotron.png.

http://www.ati.ac.at/index.php?id=247 .

http://cnx.org/contents/ezLPSYsp@1/A-Practical-Introduction-to-X.-

http://scraptirenews.com/images/charts/sieve.jpg.

http://www.iuss.org/19th%20WCSS/Symposium/pdf/0180.pdf , 2010.

http://www.nrcs.usda.gov/wps/portal/nrcs/detail/soils/ref/?cid=nrcs142p2_054223.

http://www.nrcs.usda.gov/Internet/FSE_DOCUMENTS/nrcs142p2_053264.pdf .

https://en.wikipedia.org/wiki/Soil_organic_matter .

http://www.azomining.com/images/Article_Images/ImageForArticle_160%286%29.jpg.

http://www.horiba.com/scientific/products/x-ray-fluorescence-analysis/tutorial/xrf-spectroscopy./

http://lab-training.com/2013/05/08/introduction-to-aas-component-parts./

http://crustal.usgs.gov/laboratories/icpms/intro.html.

http://biochem.pepperdine.edu/dokuwiki/lib/exe/fetch.php?media=chem331:icp-ms.jpg .(

http://chemwiki.ucdavis.edu/Core/Physical_Chemistry/Spectroscopy/Xray_Spectroscopy/XANES%3A_Theory.

http://dragon.lv/exafs/akuzmin/papers/ak65eng.pdf.

http://www.chem.ucalgary.ca/research/groups/faridehj/exp.pdf.

http://www.esrf.eu/about/synchrotron-science/history-synchrotron.

http://www.esrf.eu/about/synchrotron-science/synchrotron.

http://chemwiki.ucdavis.edu/Core/Physical_Chemistry/Spectroscopy/Xray_Spectroscopy/XANES%3A_Theory.

http://www.ung.si/~arcon/xas/xanes/xanes.htm.

http://chemwiki.ucdavis.edu/Core/Physical_Chemistry/Spectroscopy/Xray_Spectroscopy/EXAFS%3A_Theory.

الكشف عن تلوث التربة بالعناصر الثقيلة في تربة مأخوذه من مناطق من فلسطين

عادل عبد الحليم بشر

بأشراف الدكتور سلمان محمد سلمان و الدكتور مسعود حرفوش

الملخص

تشكل التربة عنصرا حاسما في البيئات الريفية والحضرية، وفي كلا المكانين تعاني التربة من تلوث كبير بفعل انشطة الانسان المختلفة . هذه الدراسة تهدف الى البحث في تلوث التربة من ثلاث مناطق في فلسطين ، حيث تم تحليل عدد كبير من عينات التربة مأخوذه من منطقة الخليل واريحا وقلقيليه ، لتقييم أثر التحضر والصناعة في تلوث التربة ، حيث تم تحليل هذه العينات باستخدام المطياف الكتلي البلازمي بالتقارن الحثي (ICP-MS)، حيث وجد ان الكروم (Cr) والزنك (Zn) موجودة بتركيزات أعلى من الحد الأقصى المسموح بها حسب منظمه الصحة العالمية (WHO) . فقد اظهرت التحاليل للتربة التي اخذت من مواقع من أريحا تلوثا بالكروم مع تركيز يصل 548 جزء في المليون، ايضا الزنك وجد بتراكيز عالية تصل في المعدل الى 452 جزء في المليون . اما التربة التي اخذت من مواقع من قلقيلية فأظهرت تلوثا قليلا بالكروم بتراكيز تصل 110 جزء في المليون. وعلى عكس من ذلك، فان التربة التي أخذت من مواقع من الخليل لم يظهر بها اي تلوث بالكروم ولا حتى بالزنك وفقا للمعايير التي وضعتها منظمة الصحة العالمية.

بالاضافه الى ذلك تم استخدام تقنيه التشكيل الدقيق لامتصاص الاشعة السينية من اجل الكشف عن البيئه المحيطه بكل من العناصر الكروم والزنك والمنغنيز الموجوده في عينات التربة ،من خلال تحليل البيانات الاولية لامتصاص الاشعة السينه اظهرت النتائج وجود ذرات الكربون(C) والفوسفور(P) حول ذرات الزنك مما يدل على شكل عضوي للزنك في التربة . بالمقابل وجد ان الكروم محاط بذرات من المنغنيز مما يعني تواجد الشكل غير العضوي للكروم في التربة. وقد وجد الكروم في حالة اكسدة تساوي 3 (Cr (III)) مما يؤدي إلى الحد من ضرر الكروم في التربة. أما المنغنيز فقد أظهرت الدراسة وجوده بشكله العضوي محاطا بذرات من الكربون. وقد وجد المنغنيز في حالة أكسدة 3 و4 (Mn_{III}, Mn_{IV}) مما يقلل تنقله وضرره في التربة أيضا.